Review

A Review on the Rheological Properties of Polystyrene/Carbon Nanotubes Composites: Fundamentals, Preparations, and Interaction Mechanisms

Saba Yaqoob , Zulfiqar Ali * , Sajjad Ali , Alberto D'Amore *

Posted Date: 26 November 2024

doi: 10.20944/preprints202411.1997.v1

Keywords: Carbon Nanotubes (CNT); Polystyrene (PS); Composite Materials; Rheological Properties

Review

A Review on the Rheological Properties of Polystyrene/Carbon Nanotubes Composites: Fundamentals, Preparations, and Interaction Mechanisms

Saba Yaqoob [1,2], Zulfiqar Ali [1,2,*], Sajjad Ali [3] and Alberto D'Amore [2,*]

[1] Dipartimento di Matematica e Fisica, Universit`a degli Studi della Campania "Luigi Vanvitelli", 81100, Caserta, Italy
[2] Dipartimento di Ingegneria, Universit`a degli Studi della Campania "Luigi Vanvitelli", Via Roma 29, 81031 Aversa, Italy
[3] Department of Physics, Government College University Faisalabad, 38000, Pakistan
* Correspondence: zulfiqar.ali@unicampania.it (Z.A.); alberto.damore@unicampania.it (A.D.); Tel.: +39-081-501-0291

Abstract: This review focuses on the rheological behavior of polystyrene (PS) composites reinforced with carbon nanotubes (CNT), providing an in-depth analysis of how CNT incorporation affects these materials' viscosity, elasticity, and flow properties. The review covers fundamental aspects of PS and CNT structures, emphasizing their influence on the composite's rheological properties. Key interaction mechanisms, including Van der Waals forces and covalent bonding, are discussed for their role in determining material behavior. Various preparation methods, such as melt, solution, and in-situ polymerization, are evaluated based on their impact on CNT dispersion and rheological performance. The study examines critical rheological parameters such as relative and complex viscosity, shear thinning, and elasticity, supported by theoretical models and experimental findings. The review also identifies major challenges, such as achieving uniform CNT dispersion and addressing processing limitations, while offering insights into future research directions to improve the rheological performance and scalability of PS/CNT composites for advanced applications.

Keywords: carbon nanotubes (CNT); polystyrene (PS); composite materials; rheological properties

1. Introduction

Polymer composites have experienced significant development over the years, rising as versatile materials with various applications in several industries e.g., construction, aerospace, automobiles, electronics, and medical [1]. Polymer composites are multifunctional materials with two or more different constituents such as polymer matrix and additives or reinforced fillers. These components synergistically merge to create a new composite material with advanced and enhanced mechanical, electrical, and thermal properties compared to the original component [2]. The integration of carbon nanotubes (CNT) into polymer matrices has revolutionized the field of material science, leading to the development of advanced composites with exceptional properties due to their unique cylindrical nanostructures composed of rolled-up graphene sheets, exhibiting extraordinary mechanical, electrical, and thermal properties. Polystyrene (PS), an extensively used thermoplastic polymer, is valued for its low cost, ease of processing, excellent electrical insulation properties, and chemical resistance, making it suitable for various applications, from packaging materials to electronics. However, despite these advantages, PS has significant limitations, including relatively low mechanical strength, poor thermal stability, and limited electrical conductivity, which restrict its use in more demanding applications. CNT incorporation into PS matrices imparts remarkable properties enhancement to overcome these limitations. Due to their high aspect ratio, CNT improves thermal and electrical conductivities and strength, making the PS/CNT nanocomposite highly suitable for demanding applications in aerospace, electronics, automotive, packaging, and other industrial sectors [3–5]. However, integrating the CNT induces substantial changes in the rheological behavior

 doi:10.20944/preprints202411.1997.v1

of the composite, increasing the viscosity, altering the shear-thinning characteristics, and increasing the nanocomposite's elastic modulus and mechanical strength. The rheological changes have critical implications for the material's processing techniques [6], requiring advanced techniques to achieve uniform CNT dispersion and prevent defects that could undermine the material's integrity. In electronics and packaging, where precision and consistency are crucial, understanding and controlling these rheological properties is essential to ensure that the composites perform as intended. Therefore, a comprehensive understanding of the rheological behavior of PS/CNT composites is indispensable in their design and fabrication, as it directly influences processability, performance, and reliability across these diverse and demanding applications [5–7].

This review paper aims to thoroughly understand the rheological properties of polystyrene/carbon nanotube (PS/CNT) composites, exploring their fundamental characteristics, interaction mechanisms, and preparation methods. By synthesizing existing research and highlighting critical challenges, we hope to offer valuable insights that can inform future studies and advancements in this rapidly evolving field. Ultimately, our work seeks to serve as a foundational resource for researchers aiming to enhance the performance and applicability of PS/CNT composites in various industrial domains.

2. Fundamentals of PS/CNT Composites

2.1. Structure of Polystyrene (PS)

Single-walled Polystyrene is a versatile and widely used thermoplastic polymer, recognized for its rigidity, ease of processing, and cost-effectiveness. It comprises repeating styrene monomers, each containing a vinyl group attached to a benzene ring. The molecular structure of PS, with bulky phenyl groups along its carbon backbone, gives it a distinct glassy and brittle nature at room temperature. This brittleness is due to the steric hindrance created by the phenyl groups, which restrict the rotational freedom of the polymer chains, resulting in a rigid material. Polystyrene can exist in both amorphous and semi-crystalline forms, although the commercially important form is typically amorphous. The amorphous nature of PS is responsible for its transparency, making it ideal for applications such as food packaging, optical lenses, and laboratory equipment where clarity is important.

Figure 1. Chemical structure of polystyrene (left), polystyrene pellets used in manufacturing (center), and expanded polystyrene foam used in packaging applications (right).

PS has several types, each with specific properties tailored to different applications. The most common form is General Purpose Polystyrene (GPPS), crystal polystyrene. GPPS is transparent, hard, and brittle, making it suitable for items such as disposable cutlery, CD cases, and other products where clarity is desired. However, its brittleness limits its impact resistance [8]. High-impact polystyrene (HIPS) was developed by blending PS with polybutadiene rubber to overcome this limitation. HIPS is opaque but offers improved flexibility and toughness, making it more suitable for applications like refrigerator linings, food containers, and toys, where impact resistance is crucial [9]. Another important type is Expanded Polystyrene (EPS), a lightweight foam version of PS produced by introducing a blowing agent that creates air pockets within the polymer. EPS is a highly effective

 doi:10.20944/preprints202411.1997.v1

insulator commonly used in packaging materials, disposable food containers, and building insulation. Its lightweight nature and thermal insulation properties make it indispensable in packaging and construction industries [10]. Extruded Polystyrene (XPS), a similar foam product, is created through an extrusion process, which results in a denser and more uniform structure. XPS has superior moisture resistance and compressive strength compared to EPS, making it particularly suitable for demanding applications like foundation insulation and roofing in construction [11]. A more specialized form of PS is Syndiotactic Polystyrene (SPS) [12], which has a unique molecular arrangement where the phenyl groups alternate systematically along the polymer chain. This configuration imparts a high degree of crystallinity, giving SPS better mechanical strength, thermal stability, and chemical resistance than PS's amorphous form. As a result, SPS is used in high-performance applications, particularly in the electronics and automotive industries, where enhanced material properties are required.

Despite its wide range of applications, PS does have limitations, particularly in terms of its low thermal stability and poor impact resistance. These drawbacks have led to advanced polystyrene composites, where the polymer is reinforced with nanomaterials like single-walled carbon nanotubes (SWCNT). Such composites significantly improve polystyrene's mechanical, thermal, and electrical properties, making it more suitable for high-performance applications that demand stronger, more durable, and thermally resistant materials [3,5]. These innovations expand the utility of polystyrene beyond its conventional uses, enabling its application in fields requiring enhanced material properties.

2.2. Properties of Carbon Nanotubes (CNT)

In the CNT, on the other hand, are allotropes of carbon with a cylindrical nanostructure. They can be classified into two main types: single-walled carbon nanotubes (SWCNT), which consist of a single graphene sheet rolled into a tube, and multi-walled carbon nanotubes (MWCNT), composed of multiple concentric graphene cylinders nested within one another [13]. CNT has remarkable properties due to their unique structure, including high tensile strength, electrical conductivity, and thermal conductivity. The sp^2 hybridization of carbon atoms in CNT forms strong covalent bonds within the graphene plane, contributing to their extraordinary mechanical and electrical properties. Figure 2 shows SWCNT can exhibit three distinct configurations, i.e., armchair, zigzag, and chiral due to the varying arrangements of carbon atoms.

Moreover, MWCNT can also be categorized based on their structural arrangement into two primary models. The first is the Russian doll model, where multiple graphite sheets are rolled into concentric cylinders, one inside the other. The second is the Parchment model, in which a single graphite sheet is continuously rolled around itself, resembling a jellyroll or rolled-up newspaper. Additionally, MWCNT can exhibit mixed structures combining elements of the Russian doll and Parchment models. The high aspect ratio (length-to-diameter ratio) and large surface area of CNT are also key structural features that play a significant role in their interactions with the PS matrix [13,14].

Preprints.org (www.preprints.org) | NOT PEER-REVIEWED | Posted: 26 November 2024 doi:10.20944/preprints202411.1997.v1

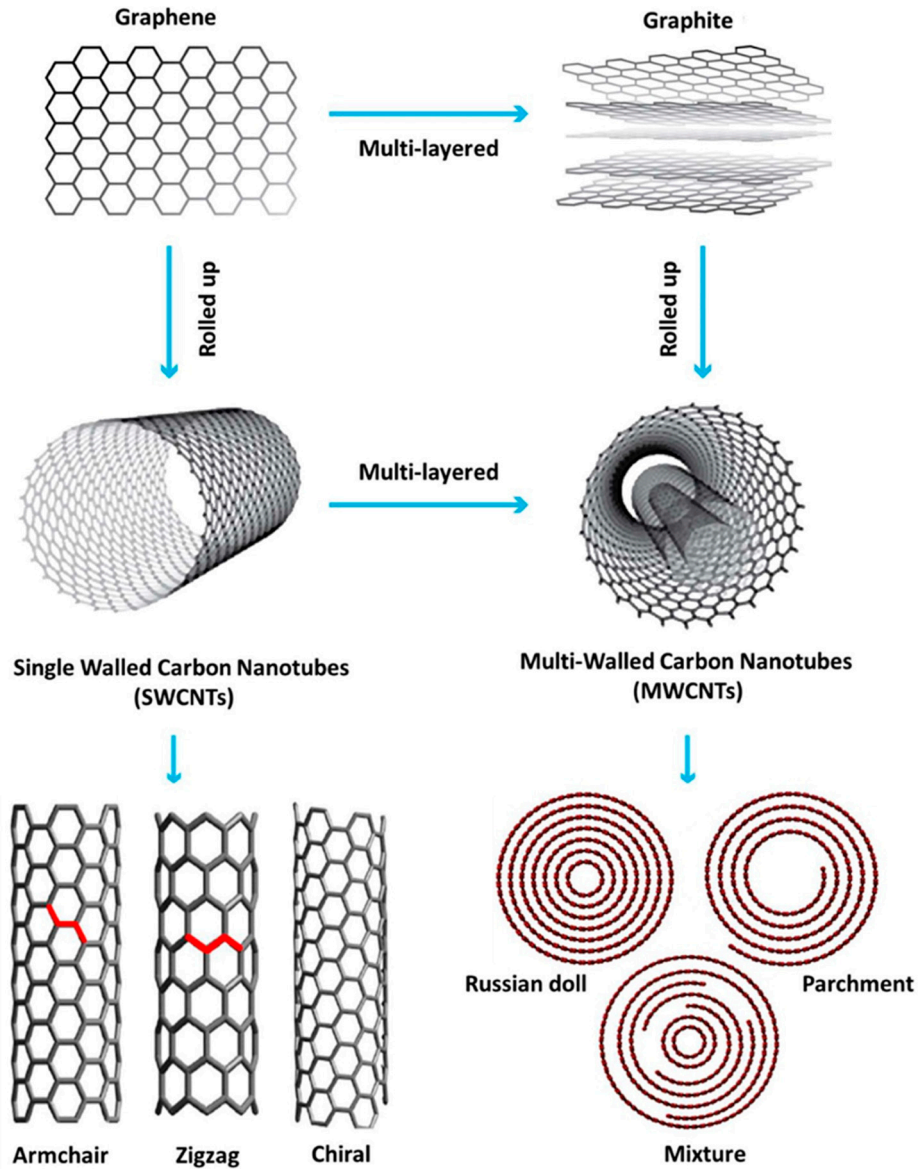

Figure 2. Overview of the formation and various configurations of SWCNT and MWCNT [13].

2.3. Interaction Mechanisms between Polystyrene (PS) and Carbon Nanotubes (CNT)

The interaction mechanisms between PS and CNT are integral to the performance of PS/CNT composites and are dictated by the physicochemical properties of both the polymer and the nanofiller. A comprehensive understanding of these interactions is essential for optimizing the composite's mechanical, thermal, and electrical properties.

2.3.1. Van der Waals Forces

Van der Waals forces are the most fundamental type of interaction between PS and CNT. These forces are weak electrostatic attractions that arise between molecules due to temporary dipoles that form as electrons move around within their orbitals. In the context of PS/CNT composites, these forces are primarily the result of interactions between the π-electrons in the aromatic phenyl rings of PS and the delocalized π-electron clouds on the surface of the CNT. Due to their high aspect ratio, the CNT's extensive surface area allows for a substantial number of these interactions to occur simultaneously, collectively contributing to a significant adhesive force between the PS matrix and the CNT [15]. This interaction is crucial for the composite's mechanical properties because, despite their weak individual strength, the cumulative effect of van der Waals forces can create a strong interfacial adhesion between the polymer chains and the CNT. This adhesion facilitates stress transfer from the PS matrix to the CNT, which is essential for improving the composite's tensile strength and

 doi:10.20944/preprints202411.1997.v1

modulus. Additionally, these interactions help maintain the structural integrity of the composite by preventing CNT aggregation, which can lead to weak points and reduce the material's overall performance. Therefore, although subtle, van der Waals forces play a foundational role in enhancing the composite's mechanical characteristics [5,16].

2.3.2.π-π. Stacking Interactions

π-π stacking interactions are another significant non-covalent interaction in PS/CNT composites, owing to the aromatic nature of both PS and CNT. These interactions occur when the aromatic rings of the PS align parallel to the graphene-like walls of the CNT, allowing the π-orbitals of the phenyl groups to overlap with the π-electrons of the CNT. This alignment leads to a stable, attractive force between the polymer and the nanofiller, enhancing the interfacial adhesion beyond what is achieved by van der Waals forces alone [5,17]. The strength of π-π stacking interactions significantly influences the mechanical properties of the composite. When the CNT is well-dispersed within the PS matrix, these interactions ensure that the polymer chains remain closely associated with the CNT under stress. This close association allows for more efficient stress transfer, thereby increasing the material's tensile strength and stiffness [18]. Moreover, the reduced mobility of the polymer chains in the vicinity of CNT, caused by strong π-π interactions, contributes to an increase in the composite's rigidity and resistance to deformation [19]. As a result, π-π stacking is a key mechanism that reinforces the composite and enhances its durability under mechanical loads.

2.3.3. Covalent Bonding

Covalent bonding, although less common in non-functionalized PS/CNT composites, represents a more robust and permanent form of interaction. This bonding can occur when CNT are chemically modified, or functionalized, to introduce reactive groups capable of forming covalent bonds with the PS chains. Functionalization typically involves attaching groups such as carboxyl (-COOH), hydroxyl (-OH), or amine ($-NH_2$) to the CNT surface, which can then react with the PS polymer during composite fabrication. This process forms a strong chemical bond between the CNT and the PS matrix, significantly enhancing the interfacial adhesion [15]. Covalent bonds in PS/CNT composites greatly improve the material's mechanical strength and thermal stability. Unlike non-covalent interactions, covalent bonds prevent slippage of the polymer chains relative to the CNT under mechanical stress, leading to a more effective load transfer and reducing the likelihood of failure under high loads [20]. Furthermore, covalent bonding can inhibit CNT aggregation, ensuring a more uniform dispersion of the nanofillers within the PS matrix. This uniformity is critical for achieving consistent mechanical and electrical properties throughout the composite. The strong bond formed through covalent interactions also increases the composite's resistance to thermal degradation, as the chemical linkages can better withstand high temperatures, making the composite more durable in demanding environments [21].

2.3.4. Dispersion and Entanglement

The dispersion of CNT within the PS matrix is a critical factor that influences the overall performance of the composite. CNT have a natural tendency to aggregate due to strong van der Waals attractions between them, leading to the formation of bundles or clusters. These aggregates can significantly reduce the effective surface area available for interaction with the PS matrix, thereby diminishing the potential improvements in mechanical and electrical properties. Achieving a uniform dispersion of CNT is challenging but essential for maximizing the benefits of their incorporation into the PS matrix [22]. Various techniques are employed to enhance the dispersion of CNT, such as sonication, mechanical mixing, and the use of surfactants or dispersing agents. Sonication, for example, uses high-frequency sound waves to break up CNT aggregates, promoting a more even distribution within the polymer matrix. Surfactants, conversely, can adsorb onto the CNT surface, reducing the van der Waals attraction between nanotubes and helping stabilize the dispersion. A well-dispersed CNT network within the PS matrix ensures that the composite exhibits uniform mechanical properties and prevents the formation of stress concentrators, which can lead to premature failure [16,19]. In addition to dispersion, the physical entanglement of polymer chains with CNT [23] plays a significant role in the composite's mechanical performance. When PS chains

 doi:10.20944/preprints202411.1997.v1

become entangled with the CNT network, this physical interaction can reinforce the composite's strength and toughness. The entanglement helps to distribute applied stress more evenly throughout the material and increases the energy absorption capacity, which is critical for improving the impact resistance and durability of the composite.

2.3.5. Interfacial Polarization

Interfacial polarization is a key factor influencing the electrical properties of PS/CNT composites, particularly when these materials are subjected to an external electric field. This phenomenon occurs between the insulating PS matrix and the conductive CNT. When an electric field is applied, the difference in electrical properties between the two materials can cause a redistribution of charges, leading to the accumulation of charges at the interface. This charge accumulation, or interfacial polarization, significantly impacts the composite's dielectric properties [19]. CNT within the PS matrix creates regions where charge carriers can accumulate, forming localized regions of high electrical potential [24]. This charge accumulation can enhance the composite's dielectric constant, making it suitable for applications requiring high dielectric materials, such as capacitors or other electronic components. The effectiveness of interfacial polarization in enhancing dielectric properties depends on the quality of the interface, which is influenced by how well the CNT is dispersed and integrated within the PS matrix [25]. Moreover, interfacial polarization can contribute significantly to the formation of conductive pathways within the composite when the CNT content exceeds a critical percolation threshold. Above this threshold, the composite transitions from an insulator to a conductor, as the CNT forms a continuous network that allows for the free flow of electrons. The alignment and connectivity of CNT, aided by interfacial polarization, plays a crucial role in determining the electrical conductivity of the composite [25]. Therefore, controlling the interfacial interactions and dispersion of CNT is essential for tuning the electrical properties of PS/CNT composites to meet specific application requirements.

3. PS/CNT Composite Preparation Methods

The formation of PS and carbon CNT composites involves integrating CNT into the PS matrix to enhance its mechanical, thermal, and electrical properties. This process requires careful control over various factors, including the dispersion of CNT, the interaction between CNT and the PS matrix, and the overall composite fabrication method. Each step in the formation of PS/CNT composites plays a critical role in determining the final properties of the material [15]. The development of PS and CNT composites has progressed significantly, evolving from traditional, straightforward methods to more sophisticated modern techniques. Each method offers unique advantages and challenges, with modern methods providing more control over composite properties and better integration of CNT into the PS matrix. Below is an exploration of traditional and modern methods, providing detailed insights into each approach.

3.1. Melt Mixing

In this Melt mixing, or melt compounding, is a widely adopted technique for producing PS/CNT composites in the polymer industry. In this method, PS pellets are melted at elevated temperatures, typically between 180°C and 220°C, within an extruder. CNT is then introduced into the molten polymer, and the mixture is subjected to high shear forces, promoting the dispersion of CNT within the polymer matrix. The molten composite is then extruded into a desired shape, which can be processed using techniques like injection or compression [26,27].

 doi:10.20944/preprints202411.1997.v1

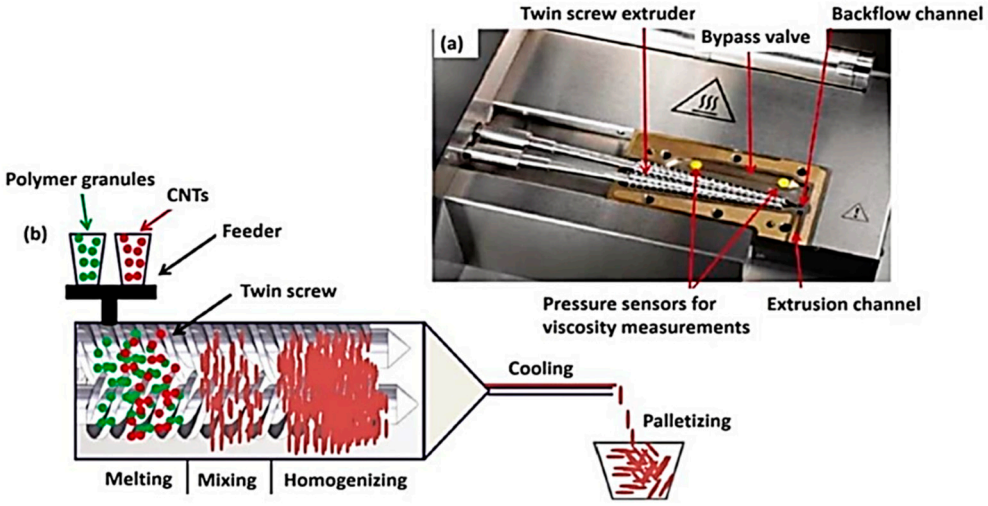

Figure 3. (a) Overview of the micro-compounder, highlighting various valves and channels; (b) schematic diagram of the twin-screw extruder used for melt mixing CNT-reinforced nanocomposites [26].

Zhang et al. [28] prepared conductive polymer composites (CPCs) by melt mixing using poly (phenylene oxide)/polystyrene (PPO/PS) blends as matrices with varying compositions. They focused on improving the dispersion of CNT by adjusting the matrix viscosity through different blend ratios. The study found that the best dispersion and electrical conductivity occurred at an intermediate matrix viscosity, which balanced polymer infiltration and CNT agglomerate breakage. Notably, the percolation threshold of the PPO/PS (35/65)/CNT nanocomposites was 63% lower than that of PS/CNT nanocomposites. Additionally, the electrical resistivity of PPO/PS (35/65)/2%CNT was approximately 10^3 Ω cm, nine orders of magnitude lower than that of PS/2%CNT.

Melt mixing is advantageous because it eliminates the need for solvents, making the process more environmentally friendly. It is also well-suited for large-scale production and is compatible with conventional polymer processing equipment. However, uniformly dispersing CNT in the viscous polymer melt is challenging, and the high processing temperatures can degrade the CNT and polymer matrix [29].

3.2. Solution Mixing

Solution mixing is one of the most used traditional methods for preparing PS/CNT composites due to its simplicity. In this method, PS is dissolved in an organic solvent, such as toluene, chloroform, or tetrahydrofuran (THF), to form a homogeneous solution. Separately, CNTs are dispersed in the same solvent using ultrasonication, which helps break down agglomerates and achieve a more uniform distribution. The PS solution and the CNT dispersion are then mixed thoroughly to ensure that the CNT is evenly distributed throughout the PS matrix. Following mixing, the solvent is evaporated under controlled conditions to produce a composite film or coating. Erkmen et al. [30] found that PS-based composites reinforced with silane-modified CNT and prepared via masterbatch dilution showed a 33% increase in tensile strength and a 34% increase in modulus compared to melt mixing. Masterbatch dilution also reduced electrical resistivity. Both methods achieved 100% shape recovery in 30 seconds during electrically actuated bending tests, highlighting improved thermal and electrical conductivity. In another study, Parnian and D'Amore [16] investigated PS/CNT nanocomposite films prepared using solution mixing and the doctor blade technique. They found that conductivity became unmeasurable with increasing CNT content in dilute PS solutions, while higher PS concentrations led to increased conductivity up to a threshold before decreasing, explained partly by PS–THF viscosity data. Sen et al. [31] demonstrated that incorporating carboxylic acid functionalized multi-walled carbon nanotubes (cMWCNT) into PS via solution blending significantly enhanced the nanocomposite (NC) films' thermal stability, rheological properties, and hardness. Figure 4 (a) shows the preparation process for PS/cMWCNT composite film. Fourier transform infrared spectroscopy (FTIR), Raman spectroscopy, and X-ray diffraction

 doi:10.20944/preprints202411.1997.v1

(XRD) confirmed the strong interaction between the PS matrix and the cMWCNT, which contributed to these improvements. Thermogravimetric analysis (TGA) showed that the well-dispersed cMWCNT increased the thermal degradation resistance of the NC films with higher activation energy and procedural decomposition temperature. Figure 4 (b) and (c) show the TEM analysis of PS nanocomposite surfaces, specifically for samples with PS concentrations of 0.3% and 0.5%, revealed a strong interfacial interaction between the PS matrix and the CNT, which appeared embedded and coiled within the matrix. The micrographs showed that the nanotubes, with diameters ranging from 12–20 nm, were uniformly dispersed in the matrix at the lower PS concentration (0.3%) Figure 4 (b). However, some regions displayed aggregated CNT masses at the higher PS concentration (0.5%) in Figure 4 (c), indicating less uniform distribution. Despite these aggregates, the overall nanotube dispersion was still good, aligning with previous findings in similar composites.

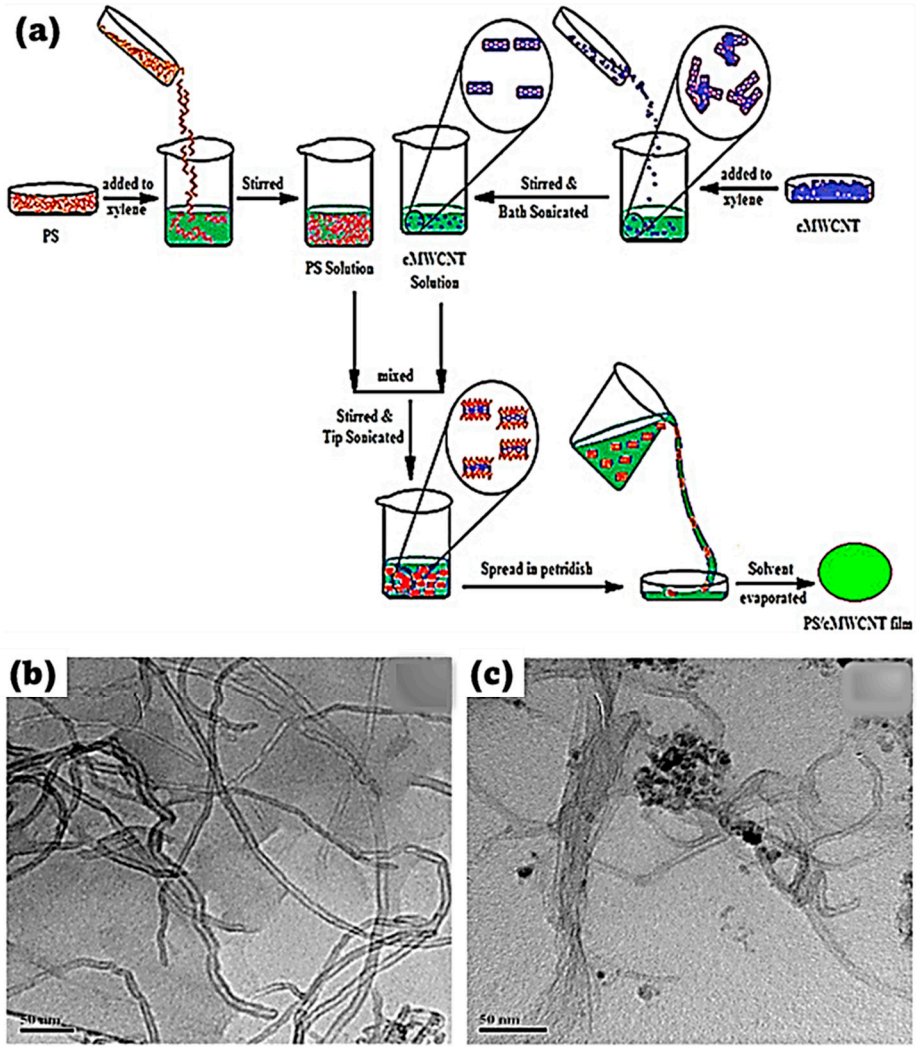

Figure 4. (a) Schematic process for PS/cMWCNT composite film preparation. TEM micrographs of PS nanocomposite surfaces show (b) a sample with 0.3% PS concentration, where the cMWCNT are uniformly dispersed within the matrix, and (c) a sample with 0.5% PS concentration, where some aggregation of cMWCNT is observed, though overall dispersion remains effective [31].

The primary advantage of solution mixing consists in its straightforwardness and effectiveness in creating thin films with dispersed CNT. However, achieving uniform dispersion of CNT remains a significant challenge due to their tendency to agglomerate. The solvent removal process can also lead to defects, impacting the composite's final properties. Despite these challenges, solution mixing has been widely used in research and small-scale production [32].

 doi:10.20944/preprints202411.1997.v1

3.3. In-Situ Polymerization

In-situ polymerization involves the polymerization of styrene monomers in the presence of dispersed CNT, allowing the CNT to be embedded within the growing PS matrix. This method can be conducted in bulk, solution, or emulsion phases, depending on the desired properties of the final composite. A polymerization initiator, such as benzoyl peroxide, is typically used to start the polymerization process. Azubuike and Sundararaj [33] explored in-situ compatibilization of polymer blend nanocomposites (PBNs) by reacting polystyrene maleic anhydride (PSMA) with nylon during melt processing. They created PS/Polyamide blends with varying PSMA (1–10 vol%) and a constant 1.5 vol% CNT loading. Adding PSMA improved CNT distribution, resulting in a conductivity of 7.4 × 10^{-2} S/m at 3 vol% PSMA, three and a half orders of magnitude higher than the non-reactive blend. The study details the mechanisms behind enhanced conductivity and improved rheological properties due to interfacial reactions. Patole et al. [34] achieved the attachment of PS nanoparticles to MWCNT via in situ microemulsion polymerization, utilizing the high surface area of selectively grown MWCNT. SEM and high-resolution (HR) TEM confirmed the distribution and anchoring of PS nanoparticles on the MWCNT surface., which enhanced the MWCNT Raman G/D ratio and increased the thermal degradation temperature of PS. The modified MWCNT exhibited improved durability and dispersibility in various organic solvents. Figure 5 (a) illustrates the proposed mechanism where MWCNT is first functionalized by anionic SDS surfactant, isolating them in water. Brownian motion causes SDS etching during polymerization, creating anchoring sites on the MWCNT for PS nanoparticles. Unanchored PS and excess SDS were removed through methanol washing, yielding the PS nanoparticle-covered MWCNT composite. Figure 5 (b) presents an SEM image of the dried composite, revealing a uniform distribution of MWCNT and PS nanoparticles. The HRTEM image in Figure 5 (c) shows spherical PS nanoparticles uniformly deposited along the length of the CNT. A closer view in Figure 5 (d) highlights the attachment of PS nanoparticles to the CNT surface. The HRTEM image in Figure 5 (e) serves as a confirmation of the proposed hypothesis.

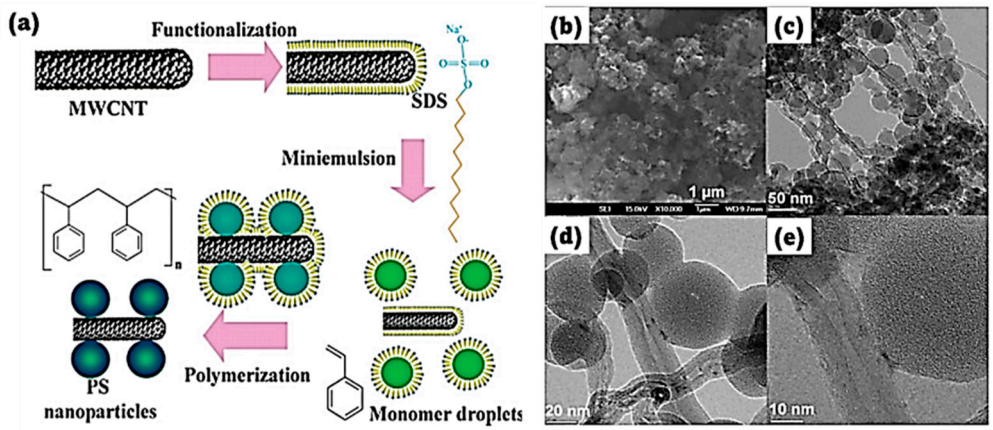

Figure 5. (a) Schematic of the multistep process for functionalizing MWCNT with PS nanoparticles via in situ microemulsion polymerization. (b) SEM and (c–e) HRTEM images of MWCNT/PS nanoparticle composites synthesized through in situ microemulsion polymerization [34].

This method offers the advantage of potentially strong interfacial bonding between the CNT and the PS matrix, which can improve the mechanical and thermal properties of the composite. Additionally, in-situ polymerization often leads to better CNT dispersion than physical blending methods. However, the process is complex and requires precise control over the polymerization conditions to prevent defects [35].

3.4. Wet Spinning

Wet spinning is a traditional technique primarily used to produce fibers or filaments from PS/CNT composites. This method extrudes a solution of PS and disperses CNT through a spinneret into a coagulation bath containing a non-solvent. The non-solvent causes the polymer to precipitate, forming solid fibers that are collected and dried. These fibers can then be drawn to improve their

 doi:10.20944/preprints202411.1997.v1

mechanical properties [36]. Farha et al. [37] developed a highly densified MWCNT yarn through wet compression using acetone, which serves as a lubricant to reduce CNT interactions and increase packing density. The yarn's density increased by 120%, from 0.211 to 0.465 g/cm³, while the diameter was controlled at 175 ± 5 μm. This process significantly enhanced the yarn's tensile strength, modulus, electrical conductivity, and gauge factor by 185%, 887.5%, 105%, and 305%, respectively. Additionally, the CNT yarn exhibited excellent electrothermal stability, reaching 275°C in 15 seconds and maintaining performance under bending and knotting, making it suitable for smart textiles, wearable electronics, and fabric heaters. Zhao et al. [38] developed a rapid and continuous twisting wet spinning method for producing highly densified CNT yarns. This process involved dispersing CNT in a surfactant solution, removing the surfactant in a coagulation bath, and applying twisting to improve yarn density and CNT alignment. The resulting CNT yarns exhibited a tensile strength of 600 MPa, Young's modulus of ≈40 GPa, and a high conductivity of 8990 S cm^{-1}.

Additionally, the CNT yarn demonstrated an ultra-fast electrothermal response of over 1000 °C s^{-1} at a low voltage of 5 V, with stable mechanical properties during heating. This scalable approach offers a pathway for producing high-performance CNT yarns for various applications. Figure 6 (a) illustrates the rapid preparation of CNT yarns, completed within minutes. SWCNT were dispersed in water with sodium taurodeoxycholate (STDOC) and extruded into an acetic acid coagulation bath at 2 mL h^{-1} for effective coagulation and surfactant removal. The gel-like CNT yarns were then twisted to enhance density Figure 6 (b, c), exhibiting strong mechanical properties without fractures during manipulation Figure 6 (d). This efficient process enabled continuous production, as demonstrated by a single CNT yarn exceeding 20 m in length collected on a spool without breakage Figure (e).

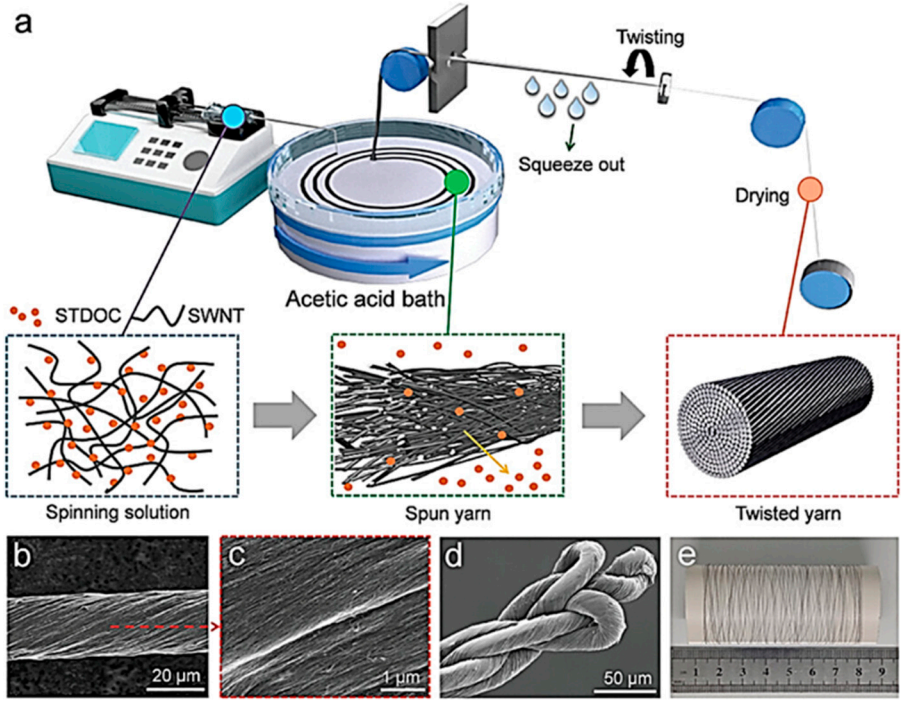

Figure 6. (a) The wet-spinning process for fabricating neat CNT yarns is depicted schematically. SWCNT particles were dispersed in water using STDOC as a surfactant and then extruded into acetic acid (coagulation bath) via a syringe to form continuous yarns. The yarn was stretched, twisted for rapid dehydration, and wound onto a spool. (b) SEM images show the CNT yarn surface. (c) A magnified SEM image highlights the neat arrangement of SWCNT. (d) The SEM image illustrates tightly intertwined, flexible CNT yarns with uniform appearances. (e) A photograph displays a 20 m long single CNT yarn wrapped on a spool without breaking [38].

Wet spinning is particularly effective for creating continuous fibers with well-aligned CNT, which can enhance the strength and conductivity of the fibers. However, maintaining uniform CNT dispersion throughout the spinning process is challenging, and the process itself is complex,

 doi:10.20944/preprints202411.1997.v1

requiring precise control of the spinning conditions. Additionally, wet spinning is associated with high equipment and operational costs.

3.5. Spray Drying

Spray drying is used to produce PS/CNT composite powders. The process involves atomizing a solution of PS and dispersing CNT into fine droplets, which are then dried rapidly in a heated chamber. As the solvent evaporates, composite particles are formed and collected as a fine powder, which can be further processed into films, coatings, or molded parts. Prasad et al. [39] introduced a straightforward spray coating method for fabricating ultraviolet (UV) and thermally stable PS-MWCNT superhydrophobic coatings. The addition of MWCNT enhanced micro/nano roughness, leading to protrusion-like surface structures. The coatings demonstrated superhydrophobic stability up to 250 °C and transitioned to superhydrophilic at 300 °C. They maintained superhydrophobicity after 50 hours of UV irradiation and water immersion. Thermogravimetric analysis revealed a 10 °C shift to higher temperatures with MWCNT incorporation, indicating weak interactions between PS and MWCNT, supported by Fourier transform infrared, Raman, and X-ray photoelectron spectroscopy. These coatings exhibit considerable potential for various applications. Zhou et al. [40] developed a novel technology for preparing styrene-butadiene rubber (SBR)/CNT composites by combining a spray drying method with subsequent mechanical mixing. The cross-linking degree of the vulcanized composites increased with the CNT content, leading to significant enhancements in mechanical properties: tensile strength improved by nearly 600%, tear strength by 250%, and hardness by 70% compared to pure SBR composites. This approach effectively reinforced the composites, demonstrating its potential to enhance the modification and reinforcement of nanocomposites with high CNT content. Figure 7 shows the schematic steps involved in the spray drying method.

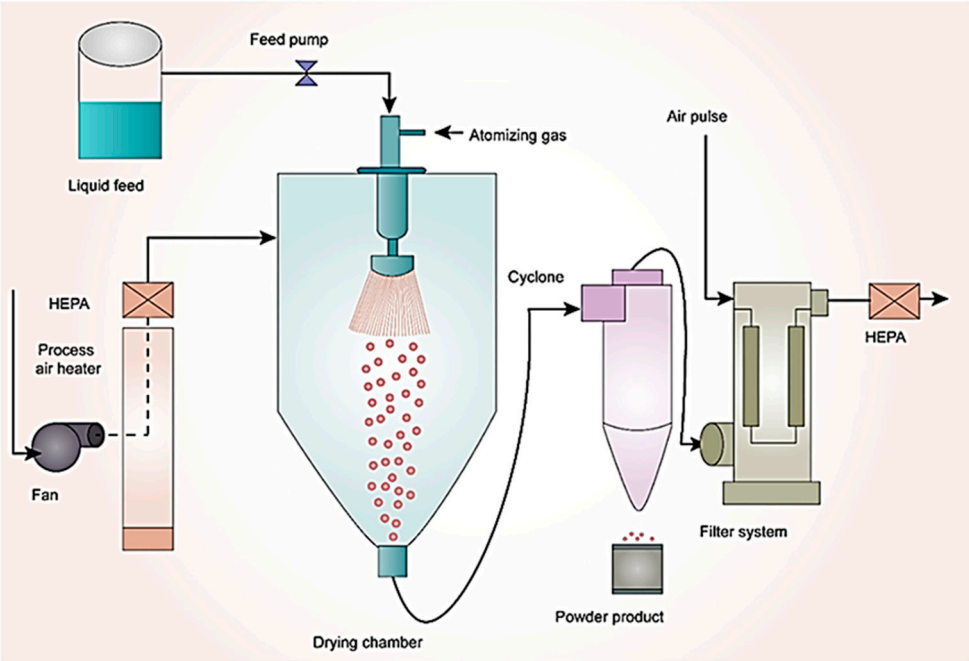

Figure 7. Schematic illustration of the spray drying process [41].

The spray drying process is advantageous for its rapidity and scalability, making it suitable for large-scale production. It also allows for control over the size and morphology of the composite particles. However, achieving uniform CNT dispersion within each particle is challenging, and the high temperatures used during drying can cause CNT agglomeration or degradation [42].

3.6. Electrospinning

Electrospinning is a modern technique for producing PS/CNT composites in nanofibers. In this method, a solution of PS and CNT is pumped through a fine needle under the influence of a high-

 doi:10.20944/preprints202411.1997.v1

voltage electric field. The electric field stretches the polymer solution into fine jets, solidifying into nanofibers as the solvent evaporates. These nanofibers are collected on a grounded collector, forming either a nonwoven mat or aligned fibers. Byun et al. [43] reported a CNT-embedded PS/PAN (6:4) nanofibrous oil sorbent using electrospinning to improve reusability and oil removal. Adding 0.25 wt.% CNT enhanced the sorbent's hydrophobicity, oleophilicity, and porosity. The sorbent demonstrated high oil absorption capacities—248 g/g for motor oil and 80 g/g for diesel oil—and retained over 70% recovery efficiency after seven reuse cycles with diesel oil. This durable, reusable sorbent shows significant promise for tackling marine oil spills. Parangusan et al. [44] developed CNT-reinforced PS nanocomposite membranes via electrospinning and enhanced polymer-filler interactions through gamma irradiation. The membranes showed optimal hydrophobicity, oil absorption, mechanical strength, and antibacterial activity at 0.5 wt.% CNT concentration and a 15 kGy irradiation dose. These findings demonstrate the membrane's potential for treating oil-contaminated water. Figure 8 provides a schematic representation of the entire procedure.

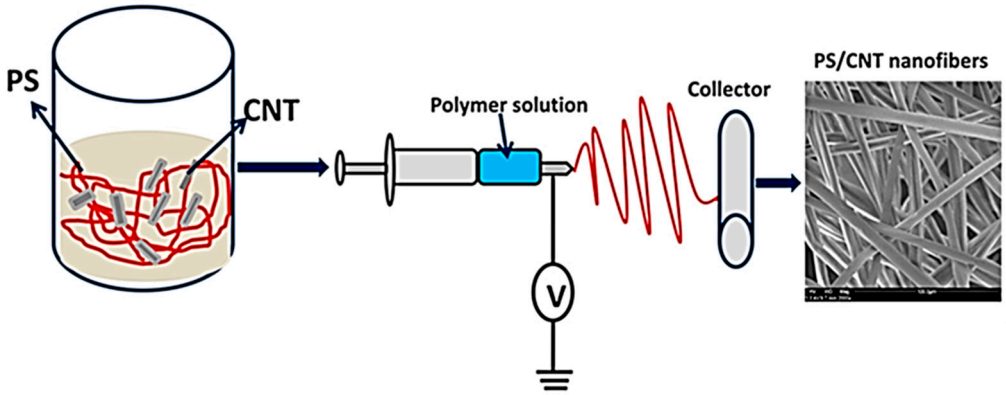

Figure 8. Schematic representation of the electrospinning process used for fabricating CNT-reinforced PS nanocomposite membranes [44].

The key advantage of electrospinning is its ability to produce nanofibers with a high surface area, which can significantly enhance the mechanical and electrical properties of the composite. Additionally, electrospinning allows for precise control over the fiber diameter and alignment, making it suitable for producing highly conductive and strong composite materials. However, the scalability of electrospinning is limited, and maintaining uniform CNT dispersion in the spinning solution is challenging. Furthermore, the process requires high-voltage equipment and efficient solvent management, adding complexity and cost.

3.7. Self-Assembly Techniques

Self-assembly techniques are modern methods that utilize the spontaneous organization of CNT and PS into ordered structures through non-covalent interactions, such as van der Waals forces or π-π stacking. In this method, functionalized CNT is mixed with PS or its monomer in a solvent, allowing the system to self-organize under controlled conditions. Factors such as solvent evaporation, phase separation, or changes in environmental conditions (e.g., pH or temperature) influence the self-assembly process, forming nanostructured composites. Oliveira et al. [45] utilized a supramolecular self-assembly approach to incorporate MWCNT into polystyrene PS nanocomposites via melt extrusion and injection molding. They investigated the effects of grafted, pristine, and carboxylated MWCNT on the morphology and mechanical properties. The self-assembly of grafted MWCNT enhanced dispersion and interfacial interactions, significantly improving mechanical performance. Electron microscopy and impact tests showed that these interfacial interactions govern crack propagation. The PS-grafted MWCNT composites exhibited an increased elastic modulus, demonstrating the effectiveness of self-assembly in creating enhanced materials for industrial applications. Liu and Wang [46] used a self-assembly method in THF to organize polystyrene (PS)-grafted MWCNT into bundles. PS grafted via atom transfer radical polymerization improved dispersibility, unlike unmodified MWCNT. The self-assembled structures

 doi:10.20944/preprints202411.1997.v1

were 15–25 μm long and 1.5–4 μm wide, with aligned nanotubes. The process was driven by solvent-philic/solvent-phobic interactions, and buoyancy and gravity influenced the final structure. A micro-phase separation model was proposed to explain this behavior. Zhang et al. [47] developed a method for creating core-shell nanospheres with PS as the core and MWNTs as the shell using hydrogen-bonding self-assembly. PS–COOH nanospheres were synthesized via soap-free emulsion copolymerization, while MWNTs were functionalized with poly (vinyl pyrrolidone) (PVP).

The carbonyl groups in PVP formed hydrogen bonds with the carboxyl groups on PS, enabling rapid and reversible self-assembly that pH can control. These core-shell nanospheres are promising as conductive reinforcement fillers in high-performance nanocomposites. Song et al. [48] developed carbon nanotube rings (CNTR) coated with gold nanoparticles (CNTR@AuNPs) using a self-assembly method. These nanostructures, with CNTR embedded in closely attached AuNPs, act as efficient Raman probes and photoacoustic (PA) contrast agents for imaging-guided cancer therapy. CNTR@AuNPs exhibited a 120-fold increase in extinction intensity at 808 nm and a 110-fold stronger SERS signal compared to CNTR, due to enhanced coupling with the AuNPs. These properties were successfully applied in cancer imaging and therapy, supported by numerical simulations and analysis. The detailed process is shown in Figure 9.

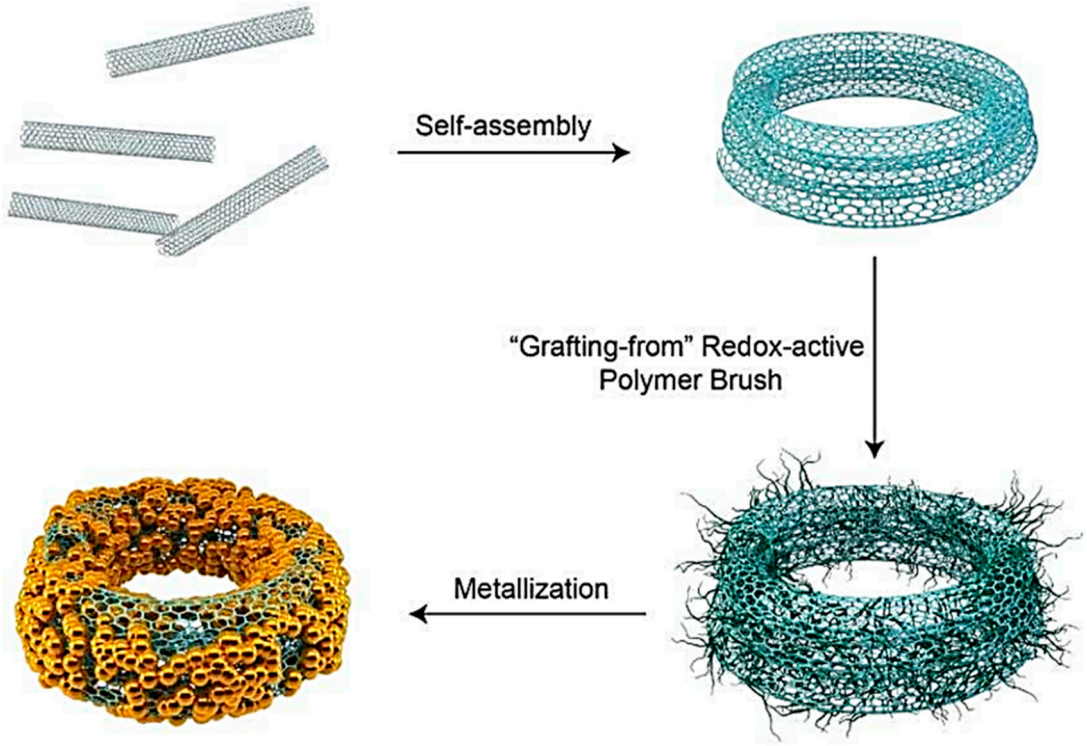

Figure 9. Schematic illustration of the self-assembly of carbon nanotubes (CNT) into CNT rings (CNTR) and the subsequent growth of redox-active poly(4-vinylphenol) (PvPH) brushes via surface-initiated atom-transfer radical polymerization (SI-ATRP) to reduce Au^{3+} to Au^{0} and coat gold nanoparticles onto the CNTR [48].

Self-assembly techniques allow for the creation of composites with precise nanostructures, which can enhance their mechanical, electrical, and thermal properties. This method is particularly advantageous for applications requiring highly specialized composite architectures. However, the process is slow and requires meticulous control over the conditions, making it difficult to scale for industrial production [15].

3.8.3. D Printing (Additive Manufacturing)

3D printing, or additive manufacturing, is an advanced technique for fabricating PS/CNT composites with complex geometries and tailored properties. In this method, PS/CNT composites are

 doi:10.20944/preprints202411.1997.v1

either prepared as a filament for Fused Deposition Modelling (FDM) or as a resin for Stereolithography (SLA). In FDM, the composite filament is heated and extruded through a nozzle to build the object layer by layer. In SLA, a photopolymer resin containing dispersed CNT is selectively cured using a laser to form each layer of the composite. Lv et al. [49] developed high-performance electromagnetic interference shielding (EMI SE) materials using 3D printing. They created lightweight honeycomb structures with polylactic acid (PLA) as a matrix and graphene nanosheets combined with carbon nanotubes (GNs/CNT) as fillers. The optimal printed material demonstrated an electrical conductivity of 110.8 S/m and an EMI SE property of 53.5 dB, well above the commercial standard of 20 dB. The study revealed that when pore sizes are less than $\lambda/5$ of the incident wavelength, the materials achieve a favorable balance of lightweight (0.4–1.0 g/cm^3) and effective EMI SE (35–45 dB). This research paves the way for diverse architectural designs in EMI SE applications through 3D printing. Baskakova et al. [50] developed a process for producing PS filaments containing 0.0025–2 wt.% SWCNT through the extrusion of crushed PS composites. The resulting filaments exhibited high uniformity in filler distribution and no air pores. Microscopy and electromagnetic property comparisons indicated that extrusion and printing enhanced SWCNT dispersion. This method enables the creation of filaments for 3D printing with various base polymers, incorporating functional fillers up to and beyond the electrical percolation threshold.

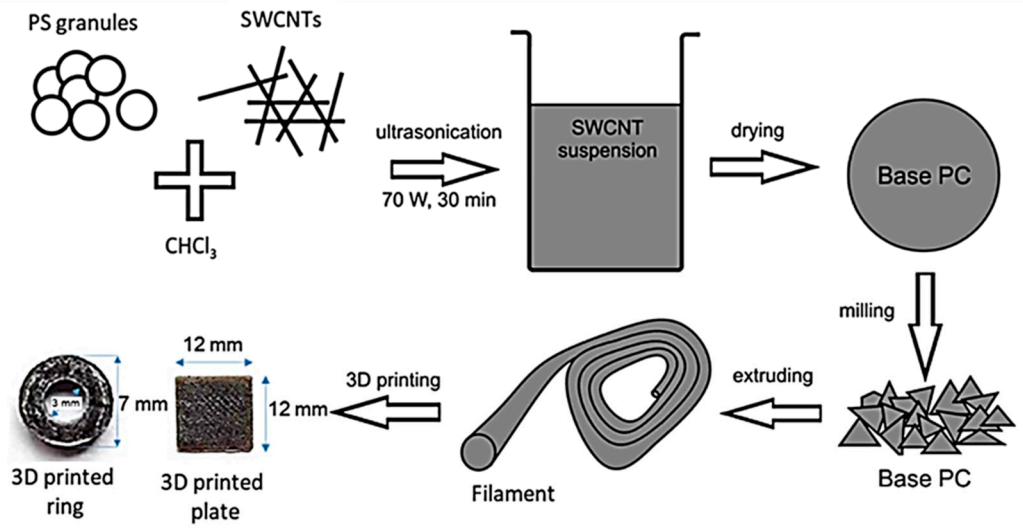

Figure 10. Comparison Schematic representation of the preparation process for base composite materials, filaments, and 3D-printed samples derived from polystyrene (PS) and single-walled carbon nanotubes (SWCNT) [50].

3D printing offers unparalleled control over the design and structure of PS/CNT composites, allowing for the creation of components with intricate internal architectures and customized properties. This method is particularly advantageous for producing functionally graded materials with varying properties within the same object. However, 3D printing has limitations, including high equipment and material costs and challenges in maintaining uniform CNT dispersion within the printing material. The process is also slower than traditional manufacturing methods, limiting its applicability for large-scale production [51].

3.9. Layer-by-Layer (LbL) Assembly

Layer-by-layer (LbL) assembly is a modern technique for creating PS/CNT composites with highly controlled multilayered structures. In this method, alternating layers of PS and CNT are sequentially deposited onto a substrate, with each layer being rinsed to remove excess material and ensure uniformity before applying the next layer. This process is repeated until the desired number of layers is achieved, resulting in a composite with a well-defined structure. Hong et al. [52] discussed LbL assembly as a versatile method for fabricating multifunctional films with tailored properties. Carbon-based nanomaterials, like carbon nanotubes and graphene sheets, are highlighted for their unique characteristics and potential in various applications, including conducting electrodes,

 doi:10.20944/preprints202411.1997.v1

batteries, solar cells, supercapacitors, fuel cells, and sensors. The article reviews the use of carbon materials in LbL-assembled nanostructured films and capsules, aiming to reveal their unique features and applications, and suggests future integration with 3D printing for enhanced functionality. Srivastava et al. [53] highlighted the LbL assembly as a cost-effective and versatile technique for creating advanced materials with structural flexibility. This method allows precise nanoscale thickness control and integrates various nanocomponents, such as nanoparticles and nanowires with polymers, enhancing their properties. The article focuses on applications of inorganic nanocrystals in polymer thin films, including the development of optomechanical materials, optical coatings, and films with strong mechanical properties. LbL assembly also shows promise in biological applications, such as neurotransmitter detection and biocompatible film fabrication. Overall, LbL assembly offers significant potential for advancing materials in both technology and biomedicine. Figure 11 explains the schematic steps involved in the LBL method.

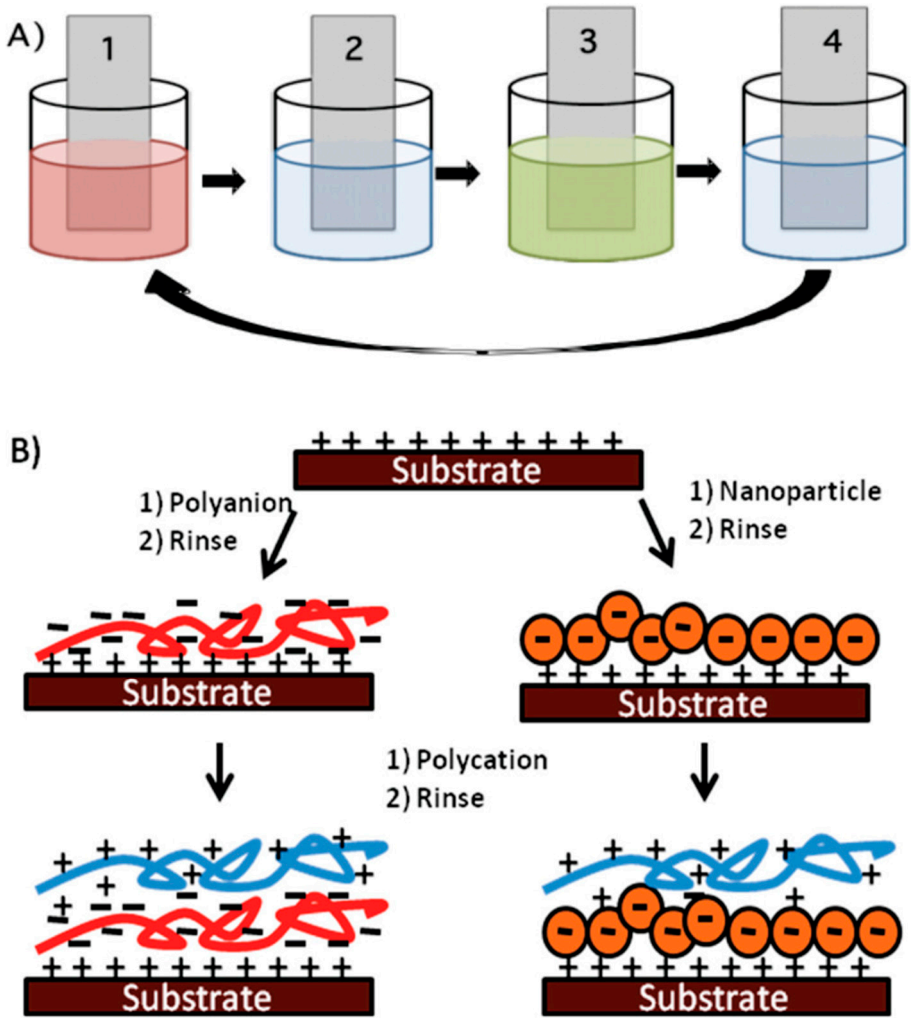

Figure 11. (A) Schematic of the layer-by-layer (LBL) film deposition process: Steps 1 and 3 illustrate the adsorption of the polyanion and polycation, while steps 2 and 4 represent the washing stages. (B) Two adsorption pathways show LBL deposition for polymers alone and for polymers with nanoparticles (NPs) [53].

LbL assembly allows for precise control over the thickness and composition of each layer, making it ideal for creating thin films or coatings with specific functional properties. This method also enables the incorporation of different types of CNT or other nanoparticles in various layers, tailoring the composite's electrical, mechanical, and thermal characteristics. However, the LbL process is slow and labor-intensive, making it less suitable for large-scale production. Despite these challenges, LbL assembly is invaluable for applications requiring highly specialized composite structures [54].

 doi:10.20944/preprints202411.1997.v1

3.10. Co-Solvent Method

The co-solvent method is a contemporary variant of solution mixing that employs multiple solvents to enhance CNT dispersion within the PS matrix. This technique involves selecting compatible solvent pairs that can improve the solubility of PS and CNT, leading to better interaction between the two phases. The process begins by dissolving PS in a primary solvent and dispersing CNT in a secondary solvent. The two solutions are mixed, and the solvents are gradually removed, typically under reduced pressure, to form the composite. By using a combination of solvents, the co-solvent method can achieve a more uniform CNT dispersion and prevent agglomeration, leading to composites with better-controlled morphologies. A study [55] explored the use of trifluoroacetic acid (TFA) as a co-solvent to improve the dispersion of MWNTs in organic solvents such as dimethyl formamide (DMF), THF, and dichloromethane. By incorporating 10 vol% TFA, effective dispersion of MWNTs was achieved without oxidation, as verified through X-ray photoelectron spectroscopy (XPS). The dispersed MWNTs were then combined with poly (methyl methacrylate) (PMMA) to fabricate nanocomposites, which exhibited excellent dispersion and low electrical percolation thresholds. These nanocomposites were further employed in organic solar cells, using a blend of SWNTs and poly(3-hexylthiophene) (P3HT) as the active layer. In the second part of the study, lithium-ion battery materials were investigated, focusing on a lithium trifluoroacetate/PMMA electrolyte system. The highest conductivity, 1.1 x 10^{-2} S/cm, was achieved at 70 wt.% salt loading using 10 vol% TFA in THF. Additionally, sol-gel-derived vanadium oxide films were examined as potential cathode materials, while a carbon nanotube/block copolymer composite was evaluated for use as an anode. The findings highlight TFA's effectiveness as a co-solvent in enhancing the properties of both polymer nanocomposites and lithium-ion battery materials. Another study by Lubineau and Rahaman [56] explored the effects of nanoscale reinforcements, particularly CNT, on the mechanical properties of continuous-fiber/epoxy-matrix laminated composites used in aerospace applications. It investigated common degradation mechanisms in laminated structures and evaluated various nano-reinforcement strategies to mitigate them. The study highlighted the role of CNT in enhancing mechanical performance due to their exceptional strength and stiffness. Additionally, it discussed the co-solvent method as a practical approach for improving the dispersion of CNT, leading to reduced degradation and enhanced performance across multiple scales.

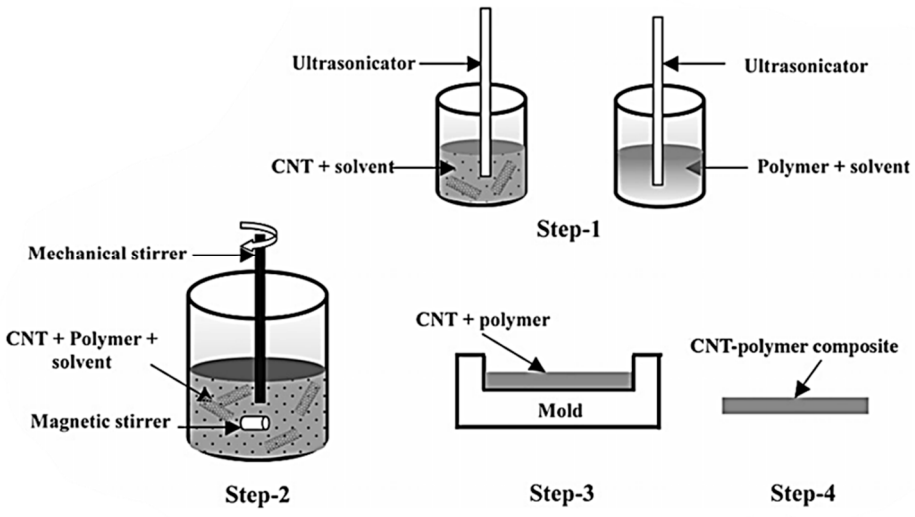

Figure 12. Schematic of the solvent casting process using a co-solvent method to prepare carbon nanotube (CNT)-polymer composites [56].

One of the significant advantages of the co-solvent method is its ability to produce composites with enhanced properties due to improved CNT dispersion. However, the method requires careful selection of solvents, as they must be compatible with both PS and CNT while ensuring effective solvent removal without leaving residues. The process also adds complexity to the preparation, as multiple solvents must be managed and removed efficiently.

 doi:10.20944/preprints202411.1997.v1

3.11. Sol-Gel Method

The sol-gel method is an advanced technique used to incorporate CNT into a PS matrix via a precursor solution that undergoes gelation and polymerization. A sol, a colloidal suspension of PS precursors and CNT in a solvent is prepared in this process. The sol undergoes a series of chemical reactions, forming a gel, a solid network that encapsulates the CNT within the PS matrix. The gel is then dried and cured to form the final composite. Liao et al. [57] presented a method for fabricating large area ordered macroporous SiO_2 inverse opals (2×2 cm^2) on ITO substrates using sequential electrophoretic deposition of PS microspheres (500 nm and 1 μm) and SiO_2 sols (~5 nm). The PS microspheres served as a template, forming a defect-free colloidal crystal. Their negative surface charge, along with that of the SiO_2 sols, enabled effective sol-gel transformation. The resulting inverse opals displayed excellent surface uniformity and structural integrity after infiltrating SiO_2 into the voids and oxidizing to remove the PS template. Fourier transform infrared spectroscopy confirmed the removal of PS, leaving a complete SiO_2 skeleton, while X-ray diffraction showed its amorphous nature. Gao et al. [58] employed a conventional sol-gel method to prepare CNT/TiO_2 nanocomposites with carbon loadings up to 20% by weight. The bare multi-walled CNT and the composites were characterized using techniques such as TEM, XRD, BET, and TGA–DSC. The results indicated successful coating of the CNT with discrete clusters of TiO_2, which, after annealing at 500 °C, formed mesoporous crystalline TiO_2 (anatase) clusters. The photocatalytic activity was assessed through the photodegradation of methylene blue (MB), revealing that the optimal CNT/TiO_2 ratio was between 1.5% and 5% by weight, leading to a maximum activity increase of 12.8% compared to pure TiO_2. In the study by Toyama et al. [59], the authors investigated the synthesis of (PS)@TiO_2 core-shell particles using the sol-gel method with an aqueous NH_3 promoter. They found that reaction temperature and promoter concentration significantly influenced particle morphology, resulting in a TiO_2 shell thickness of approximately 5 nm, as confirmed by transmission electron microscopy. The energy-dispersive X-ray spectroscopy detected titanium on the surfaces. The PS@TiO_2 particles exhibited superior photocatalytic activity in methylene blue degradation compared to commercial P25, and sol–gel synthesized TiO_2. This research highlights the sol-gel method's effectiveness in enhancing the photocatalytic properties of PS@TiO_2 core-shell structures. Lai et al. [60] investigated carbon-doped TiO_2 due to its nontoxicity, stability, and abundance, which enhance light absorption efficiency. High-efficiency photocatalysts were synthesized through a hydrothermal reaction in a high-pressure reactor, followed by the preparation of TiO_2/CNT mesoporous composites using the sol-gel method in an ultrasonic environment (Figure 13). Characterization via SEM and TEM revealed the presence of TiO_2 nanoparticles alongside CNT, with phase analysis confirming an anatase-doped structure. Tests demonstrated that these composites exhibited superior infrared and visible light absorption compared to pure TiO_2. The TiO_2/CNT mesoporous nanomaterials developed in this study show promise for clean industrial applications.

 doi:10.20944/preprints202411.1997.v1

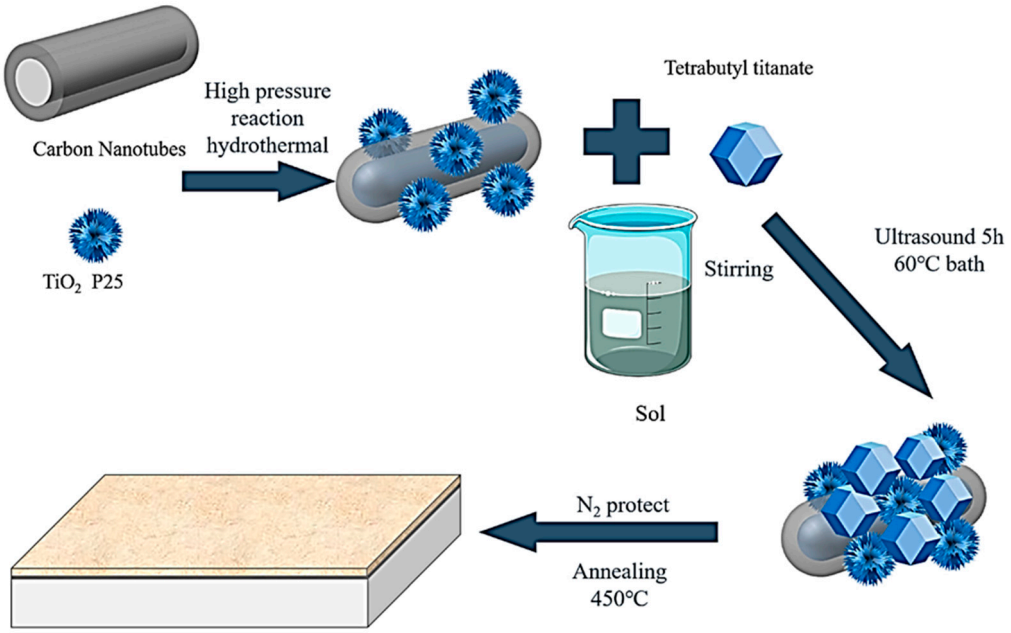

Figure 13. Schematic illustration of mesoporous TiO_2/CNT nanomaterial membrane formation using the sol-gel method with ultrasonic irradiation [60].

The sol-gel method allows for the creation of PS/CNT composites with high structural control and enhanced thermal stability due to the strong interaction between the CNT and the polymer matrix. This method also offers the possibility of tailoring the composite's properties by adjusting the sol-gel process parameters. However, the sol-gel process is complex, requiring precise control over the chemical reactions involved. The need for careful management of the gelation process makes it more suitable for specialized applications rather than routine use [61].

3.12. Microwave-Assisted Processing

Microwave-assisted processing is a modern technique that utilizes microwave radiation to enhance the preparation of PS/CNT composites. In this method, the composite mixture, typically consisting of PS and CNT, is exposed to microwave radiation, which selectively heats the CNT due to its high electrical conductivity. This selective heating improves the dispersion of CNT within the PS matrix and promotes better interfacial bonding between the CNT and the polymer. Xie et al. [62] developed lightweight, high-strength microcellular PS/CNT composite foams using a microwave-assisted foaming and welding method. The foams exhibited a density of 0.095 g/cm^3, an ultralow percolation threshold of 0.0014 vol%, and a high electromagnetic interference shielding effectiveness of 211.5 dB cm^3/g at 12.4 GHz with just 0.046 vol% CNT. Microwave sintering enhanced the compression stress to 7.1 MPa and tensile strength to 2.2 MPa. This work demonstrates the efficacy of microwave-assisted processing in creating multifunctional composite foams for wearable electronics. Xie et al. [63] presented a microwave-assisted molding technique to establish a segregated structure in poly (lactic acid) (PLA)/CNT composites, effectively enhancing the stabilization of conductive networks in low-melt-viscosity PLA (Figure 14). The CNT coating functioned as a microwave absorber, generating localized heating that precisely controlled the surface temperature of the PLA granules, facilitating optimal softening and fusion while minimizing the migration of CNT. This methodology preserved the integrity of the CNT network and improved interfacial adhesion. The resulting composite, containing only 5.0 wt.% CNT exhibited an electrical conductivity of 16.3 S/m and an impressive electromagnetic interference shielding effectiveness of 36.7 dB at 10.0 GHz. These findings underscore the potential of microwave-assisted processing for developing segregated structures in low-melt-viscosity polymers.

 doi:10.20944/preprints202411.1997.v1

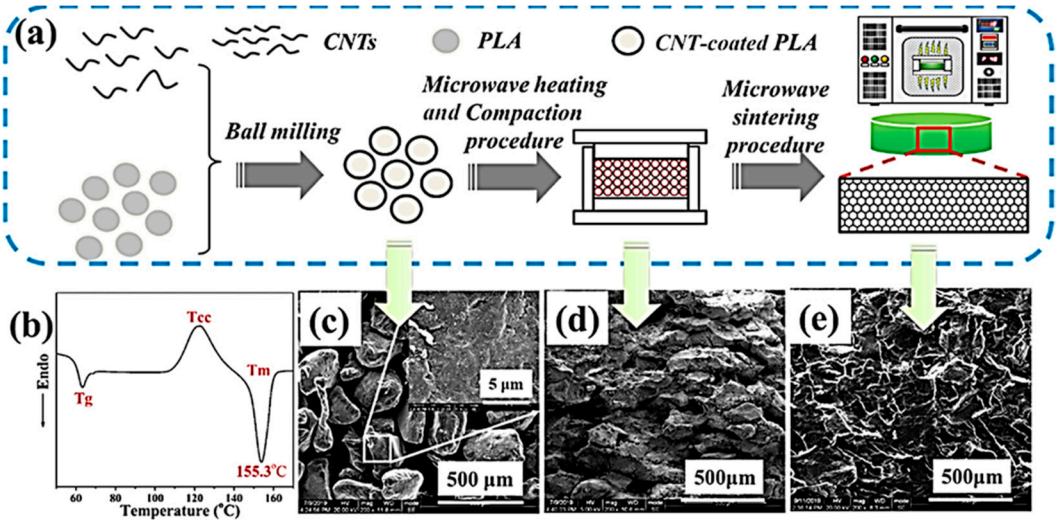

Figure 14. (a) Schematic illustration of the fabrication process for segregated PLA/CNT composites via microwave-assisted sintering. (b) Differential scanning calorimetry (DSC) curves for PLA and (c) 5 wt.% CNT-coated PLA granules, along with their surface morphology. (d) The fractured surfaces of the 5 wt.% CNT/PLA composite following the compaction procedure and (e) the sintering procedure are also presented [63].

Microwave processing offers several advantages, including energy efficiency and faster processing times compared to conventional heating methods. The technique also enhances the properties of the composite by improving CNT dispersion and reducing processing times. However, microwave-assisted processing requires careful control to prevent the degradation of materials, as excessive heating can damage both the PS matrix and the CNT [64].

3.13. Chemical Vapor Deposition (CVD) with PS Deposition

Combining Chemical Vapor Deposition (CVD) and PS deposition is an advanced method for fabricating CNT/PS composites. CNT is first grown on a substrate via CVD, where a hydrocarbon gas decomposes at high temperatures, forming CNT on metal nanoparticle catalysts like Fe, Co, Ni, or Mo. These catalysts, supported by Al_2O_3, MgO, or SiO_2 substrates, facilitate CNT growth, with hydrocarbons like CH_4, C_2H_2, or even liquid benzene and alcohol serving as carbon sources. After CNT synthesis (at 600–1100 °C), PS is deposited onto the CNT by in-situ polymerization, spin coating, or dip coating. Flexible CNT, critical for electronic applications, can be produced at lower temperatures (25–500 °C). Various CVD methods, such as thermal (TCVD) and plasma-enhanced (PECVD), have been developed for large-scale CNT production [65]. Martínez et al. [66] developed composites from PS with hydroxyl end groups and multiwall CNT to evaluate their properties. CNT was synthesized via CVD, and the PS was produced through solution polymerization. Thin films were created by pouring into petri dishes or dip-coating. Characterization included SEM, FTIR, Raman, UV-vis, Vickers microhardness, and electrical resistivity analysis. Raman spectroscopy revealed interactions between CNT and polystyrene. Results showed that resistivity and transparency decreased with increasing CNT concentrations, with transmittance at about 80% for 0.8 wt.% CNT and maximum Vickers hardness at 1.6 wt.%. Guzenko et al. [67] developed conductive polymer composites (CPCs) for flexible piezoresistive sensors using hollow three-dimensional graphitic shells (GS) as a filler in the PS matrix. Synthesized via chemical vapor deposition (CVD), the GS enhanced the piezoresistive response of the composites compared to commercial MWCNT, despite lower mechanical and thermal performance. The distribution of GS and CNT was analyzed using X-ray diffraction and scanning electron microscopy, alongside evaluations of electrical, thermal, and mechanical properties.

 doi:10.20944/preprints202411.1997.v1

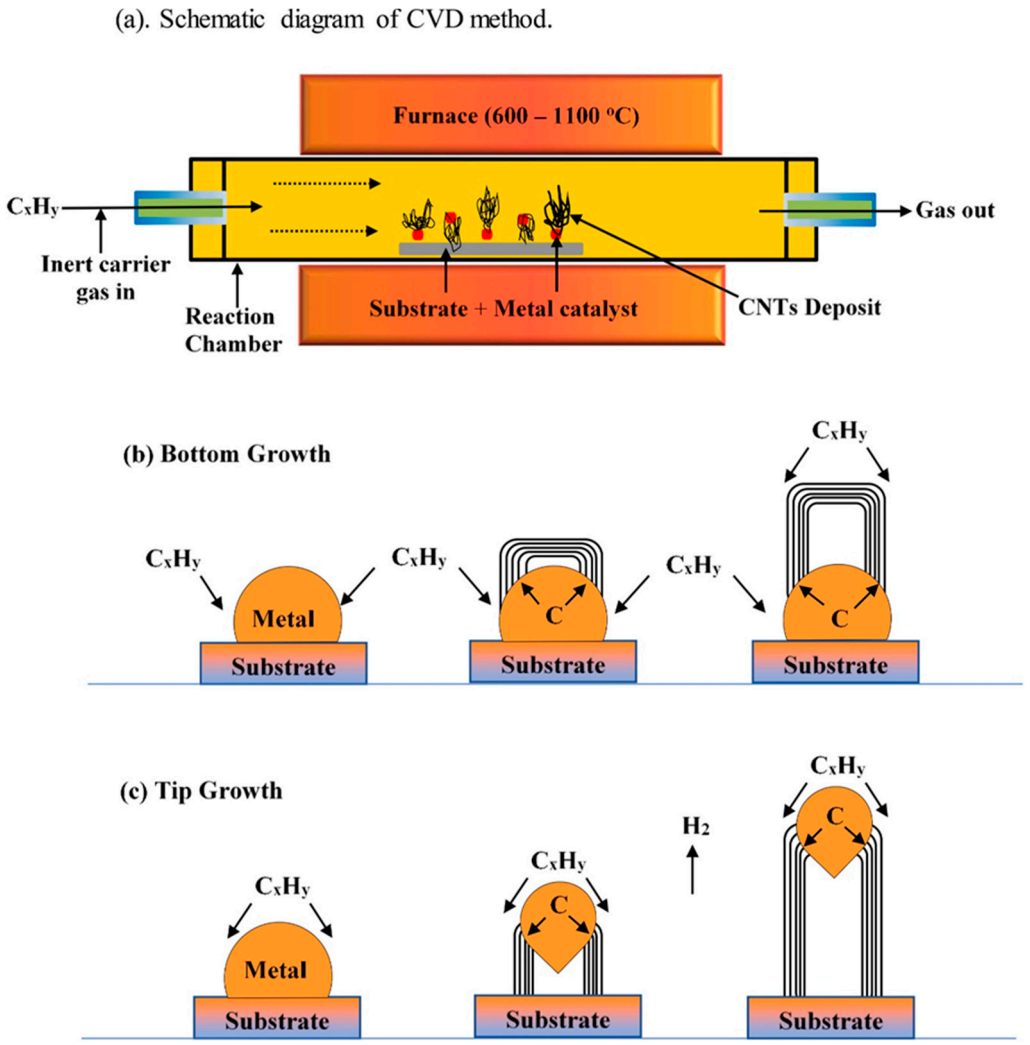

Figure 15. (a) Schematic diagram of the CVD method. (b) Growth mechanism of carbon nanotubes through bottom growth. (c) Growth mechanism of carbon nanotubes through tip growth [65].

This method ensures that CNT are well-integrated into the PS matrix, offering the potential for excellent alignment and distribution of CNT within the composite. The resulting PS/CNT composites exhibit superior mechanical, electrical, and thermal properties due to the high-quality integration of CNT. However, the CVD process is complex and expensive, typically requiring specialized equipment and conditions. As a result, this method is often used for research and specialized applications rather than large-scale manufacturing.

4. Rheological Properties of PS/CNT Composites

4.1. Relative and Complex Viscosity

The presence of CNT significantly influences the viscosity of melted PS. Viscosity measures a material's resistance to flow, and the addition of CNT can alter this property in various ways. In general, the viscosity of PS/CNT composites increases with CNT concentration due to the formation of a network of interconnected CNT within the polymer matrix. This network acts as a physical barrier to flow, increasing the composite's resistance to deformation. At low CNT concentrations, the increase in viscosity is relatively moderate, as CNT is dispersed throughout the PS matrix without significant interaction. However, as the concentration of CNT increases, the likelihood of CNT-CNT interactions rises, leading to the formation of a percolated network. This network results in a more pronounced increase in viscosity, often resulting in a gel-like or solid-like behavior at high CNT loadings. The viscosity behavior of these composites can be characterized by models such as the

 doi:10.20944/preprints202411.1997.v1

Einstein-Batchelor equation [68], which describes the relationship between viscosity and particle concentration.

The equation for the relative viscosity (η_r) in a dilute suspension is given by:

$$\eta_r = 1 + 2.5\phi \quad (1)$$

where η_r is the relative viscosity and ϕ is the volume fraction of CNT. This equation is valid for low concentrations of CNT, where interactions between particles are minimal. For higher concentrations, more complex models, such as the Krieger-Dougherty or Mooney equation, account for particle interactions and network formation [69]. Parnian and D'Amore explored how polymer solution viscosity affects carbon nanotube (CNT) dispersion, focusing on its impact on mechanical and electrical properties. They found that viscosity depends on polymer concentration and molecular weight, with distinct behaviors emerging at different concentration levels. Below a critical concentration, the polymer chains are loosely distributed, resulting in lower viscosity and minimal interaction between chains. Above this critical concentration, the chains become entangled, significantly increasing viscosity and making flow more difficult. Their findings suggest that CNT dispersions are unstable when polymer concentration is near this critical point, as network structures do not form effectively. However, increasing the concentration beyond this point leads to a sharp rise in viscosity, Figure 16, promoting the formation of more stable network structures. This indicates that viscosity is a key factor in determining the stability and uniformity of CNT dispersions, with higher viscosity aiding in achieving stable dispersions [16].

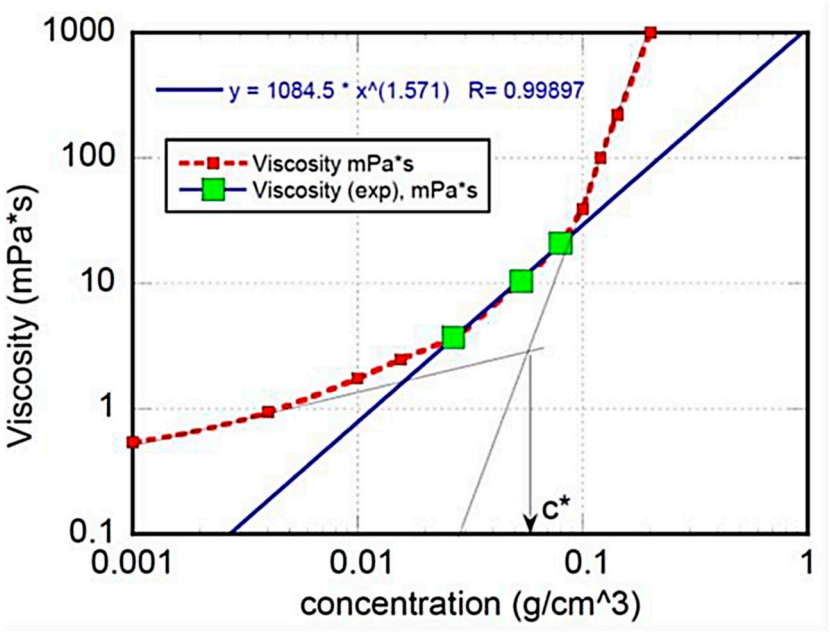

Figure 16. The "zero shear" viscosity of PS–THF solutions plotted against polymer concentration. The green symbols indicate the concentrations and viscosity ranges of the solutions used for CNT dispersions in the study. The blue line serves as a visual guide [16].

Complex viscosity (η^*) is a measure of a material's resistance to deformation under oscillatory shear. It combines the elastic and viscous components of the material's response and is useful for characterizing the overall rheological behavior of PS/CNT composites. Complex viscosity is determined from oscillatory rheometric data, providing insights into the material's viscoelastic properties.

The complex viscosity is given by:

$$\eta^* = \frac{\sqrt{G'^2 + G''^2}}{\omega} \quad (2)$$

 doi:10.20944/preprints202411.1997.v1

where G' is the storage modulus, G'' is the loss modulus, and ω is the angular frequency of the applied oscillatory stress. The complex viscosity of PS/CNT composites typically increases with CNT concentration due to the formation of a percolated CNT network, which imparts additional resistance to deformation. Analyzing complex viscosity helps in understanding the interplay between elastic and viscous behavior in PS/CNT composites. It provides valuable information for optimizing processing conditions and predicting the material's performance in various applications.

Park et al. [70] examined the rheological properties of MWCNT and PS composites, focusing on complex viscosity (η*), storage modulus (G′), and loss modulus (G″). The study considered various contents of a dispersing agent (0, 10, and 20 wt.%) with the physical gel formation and MWCNT dispersion within the composites. Although all composites displayed similar rheological trends, the results for the composite without the dispersing agent were primarily highlighted for clarity. At 210 °C, the complex viscosity (η*) versus frequency plot for the composite with 0 wt.% dispersing agent showed (Figure 17) that complex viscosity increased with higher MWCNT concentrations. This effect was most pronounced at low frequencies, where MWCNT concentrations between 2 and 5 wt.% significantly altered the frequency dependence of complex viscosity. As frequency increased, the complex viscosity decreased due to shear thinning behavior, illustrating the dynamic response of the composite material under varying shear conditions.

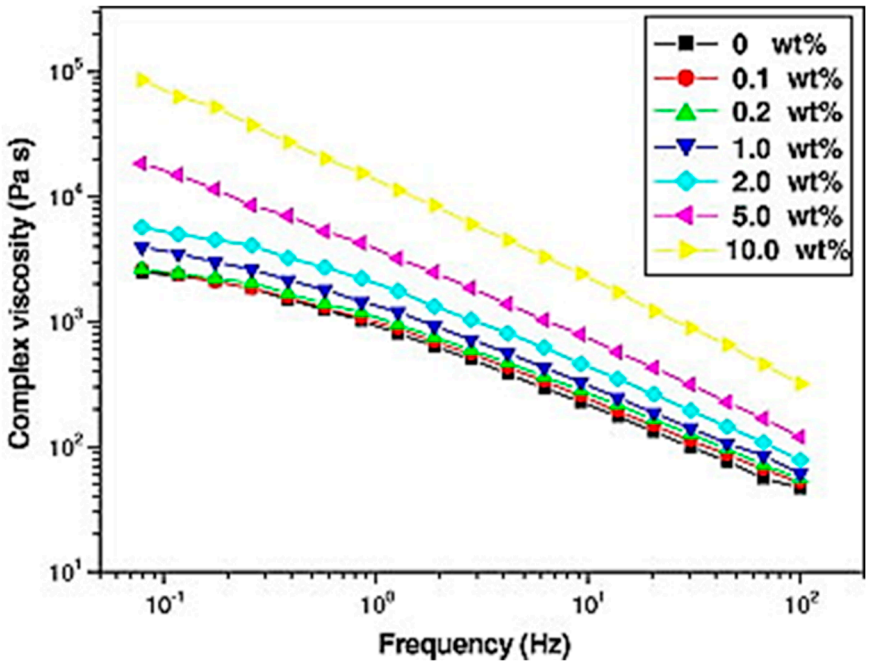

Figure 17. Complex viscosity (η*) of MWCNT/PS composites at 210 °C at various MWCNT concentrations, without any dispersing agent [70].

Kaseem et al. [15] investigated the impact of various MWCNT treatment methods on the rheological properties of latex-blended PS/MWCNT composites. They compared four treatments: untreated (PS/P-CNT), acid-treated (PS/A-CNT), ultrasonic-treated (PS/U-CNT), and a combination of acid and ultrasound (PS/AU-CNT). The findings revealed that the PS/P-CNT composites had the poorest dispersion due to weak interactions between the PS latex and MWCNT, while the PS/AU-CNT composites achieved the best dispersion. Figure 18 (a) and (b) illustrate this disparity, with Figure 18 (a) showing the poor dispersion in PS/P-CNT composites and Figure 18 (b) highlighting the optimal dispersion in PS/AU-CNT composites. Rheological analysis indicated that PS/P-CNT exhibited shear-thinning behavior, characterized by a Newtonian plateau at low frequencies and shear thinning at higher frequencies, as depicted in Figure 18 (c). Nanotube interactions formed a solid-like network at low frequencies, resulting in significant yield stress. Conversely, at higher frequencies, as illustrated in Figure 18 (d), weakened nanotube interactions and the orientation of fillers led to lower viscosities, underscoring the critical role of treatment methods in optimizing dispersion and rheological performance in the composites.

Preprints.org (www.preprints.org) | NOT PEER-REVIEWED | Posted: 26 November 2024 doi:10.20944/preprints202411.1997.v1

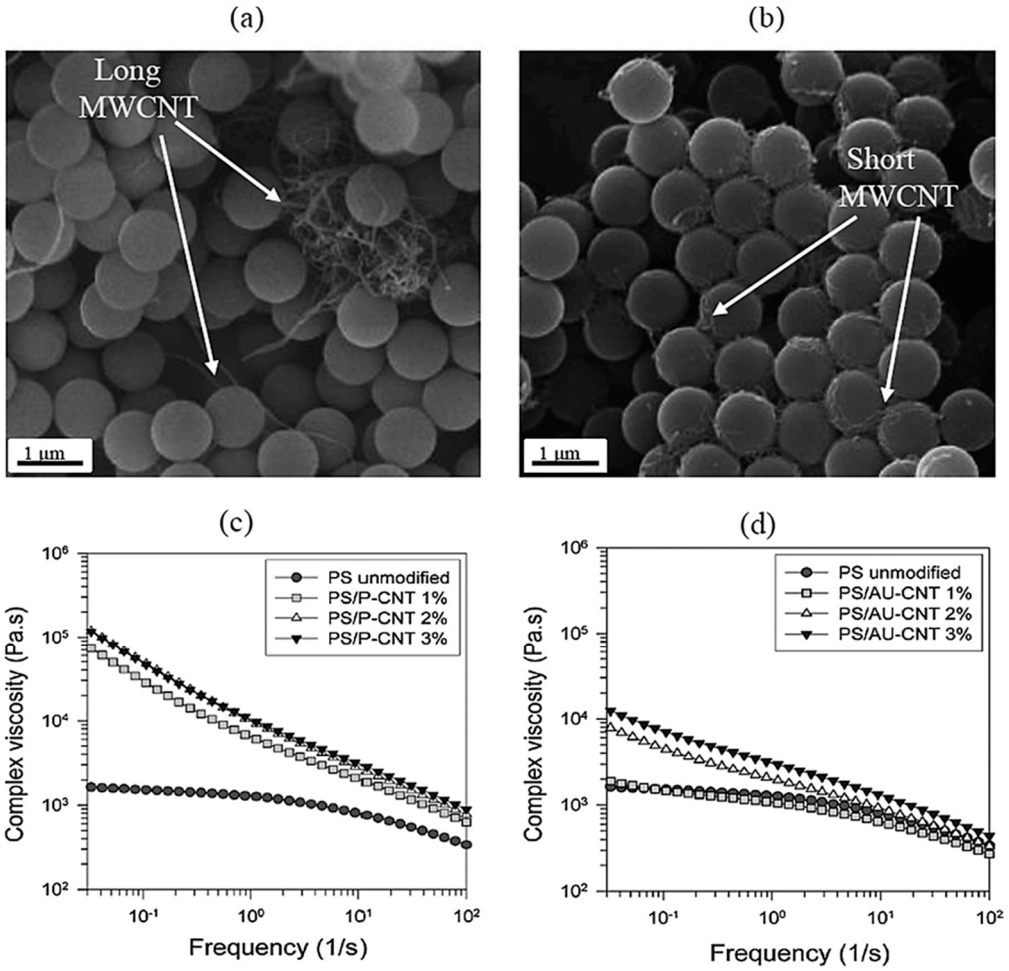

Figure 18. SEM images demonstrating the dispersion characteristics of MWCNT within freeze-dried PS/MWCNT composites: (a) PS/P-CNT and (b) PS/AU-CNT. Furthermore, (c) depicts the complex viscosities of PS/P-CNT composites at 210 °C as a function of frequency, while (d) illustrates the complex viscosities of PS/AU-CNT composites at 210 °C across the same frequency range [15].

4.2. Elasticity

Polymers and polymer composites are viscoelastic materials. They exhibit simultaneous elastic and viscous behavior since their mechanical response is strain- and strain-rate-dependent. In PS/CNT composites, Incorporating CNT enhances the material's elastic response, reflecting an increase in resistance to deformation. Dynamic mechanical analysis measures the complex modulus from which the in-phase or storage modulus (G') and the out-of-phase or loss modulus (G'') can be recovered. The storage modulus represents the material's elastic, or "solid-like," behavior, while the loss modulus represents the viscous, or "liquid-like," behavior. In the glassy state, below the glass transition temperature, T_g, and at high loading frequencies, in the melt state, the response of PS/CNT to mechanical loadings is almost completely elastic. At the same time, the loss modulus prevails in the melt and glassy states at low loading frequencies, reflecting the concept of the time/frequency-temperature superposition principle. However, incorporating CNT enhances the material's elastic part of the response, reflecting an increase in resistance to deformation. Then, at high loading frequencies and in the glassy state, where the response is prevalently elastic the following equation can describe the relationship between the elastic modulus and CNT concentration:

$$E = E_0 + k\phi^n \quad (3)$$

where E is the elastic modulus of the composite, E_0 is the modulus of the pure PS, k is a constant related to the reinforcement effect of CNT, and n is the concentration exponent. This equation highlights the significant impact of CNT on the composite's elasticity, with higher concentrations

 doi:10.20944/preprints202411.1997.v1

leading to more significant improvements in stiffness and rigidity [71]. Fragneaud et al. [72] studied the enhancement of interfacial adhesion in PS- CNT composites by grafting PS chains onto CNT surfaces. They covalently bonded polystyrene with an average molecular weight of about 104 g mol^{-1} and synthesized composites with varying CNT weight fractions. The grafting improved nanotube dispersion, increased Young's modulus below T_g, and enhanced stress at break, while low molecular weight grafting plasticized the matrix near the nanotube surface.

In Figure 19, the storage shear modulus at 420 K is plotted against filler volume fraction and compared to the Halpin-Kardos (HK) model, which does not account for the fiber-fiber interaction. For CNT fractions below 0.5 vol.%, the moduli aligned well with HK predictions. However, at higher fractions, observed moduli exceeded the HK model's prediction, highlighting the impact of nanotube entanglements on mechanical behavior, especially when the polymer acts nearly as a liquid. Additionally, PS-g-CNx composites were less stiff than a-CNx MWNT composites due to the lubricant effect of the grafted PS layer aiding nanotube disentanglement.

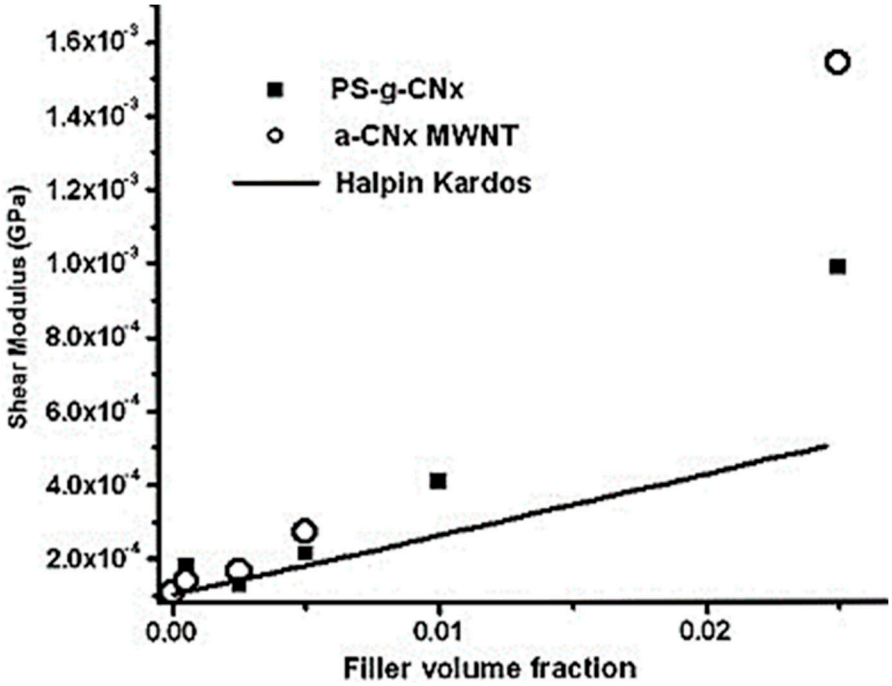

Figure 19. Shear storage modulus at 420 K of polystyrene composites filled with a-CNx MWNTs (○) and PS-g-CNx MWNTs (■), compared to the shear modulus calculated using the Halpin–Kardos equation (—) [72].

Another study [70] explored the mechanical properties of PS composites reinforced with MWCNT, focusing on the influence of MWCNT content on viscoelastic behavior. The composites' storage modulus (G′), measured at 210 °C, is logarithmically plotted as a function of frequency in Figure 20 (a). The results show that G′ generally increased with frequency, with a more pronounced rise in the storage modulus, particularly in the low-frequency range. This finding suggests a heightened sensitivity of G′ to frequency variations. Figure 20 (b) presents the G″ versus frequency. Like the storage modulus, G″ also exhibited an increase with frequency. However, the rise in G″ was less pronounced than that of G′, indicating that the storage modulus is more sensitive to changes in frequency. Additionally, a significant qualitative change in both moduli versus frequency plots was noted at T=210°C, when the MWCNT content was increased from 2 to 5 wt.%, suggesting that higher MWCNT concentrations substantially enhance the viscoelastic properties of the composites.

 doi:10.20944/preprints202411.1997.v1

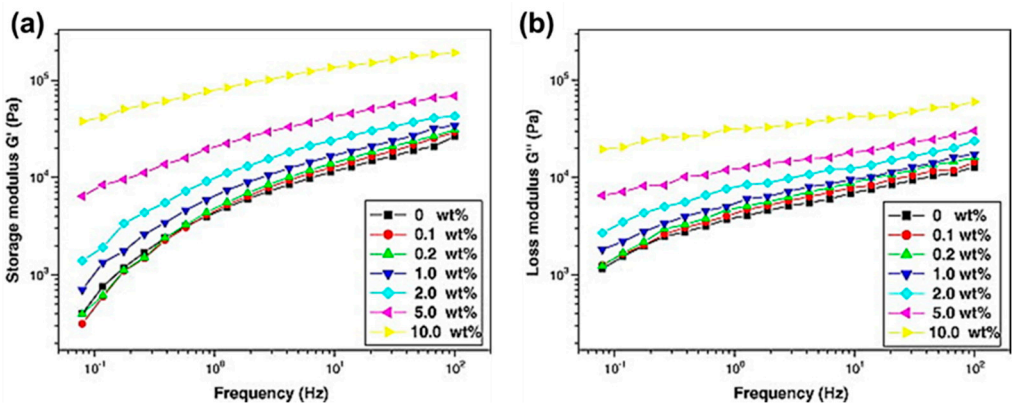

Figure 20. Storage modulus (G′) and loss modulus (G″) of MWCNT/PS composites without the dispersing agent, measured at 210 °C. (a) Storage modulus (G′). (b) Loss modulus (G″) [70].

Zhang et al. [28] developed low-cost, high-performance conductive polymer composites (CPCs) using miscible poly (phenylene oxide)/PS (PPO/PS) blends as matrices to enhance the dispersion of CNT. This approach achieved a significantly lower percolation threshold than traditional methods, resulting in improved electrical conductivity. Figure 21 illustrates the rheological properties of the composites. In (a) and (b), the G′ and G″ are shown as a function of frequency, respectively. Both G′ and G″ increase with CNT content, with a more pronounced rise in G′, indicating typical behavior for filled polymers. The substantial increase at low frequencies suggests the formation of a CNT network that enhances the composites' elasticity. In (c), the damping factor (tan δ) decreases with increasing CNT content, reflecting the development of a more elastic material. Finally, (d) displays the complex viscosity, which shows shear-thinning behavior in CNT-containing composites, indicating effective dispersion and interactions between CNT and the PPO/PS matrix. A low-frequency plateau in G′ and a positive slope in tan δ at 2.0 wt.% CNT content confirms establishing a rheological percolating network consistent with the previously determined electrical percolation threshold.

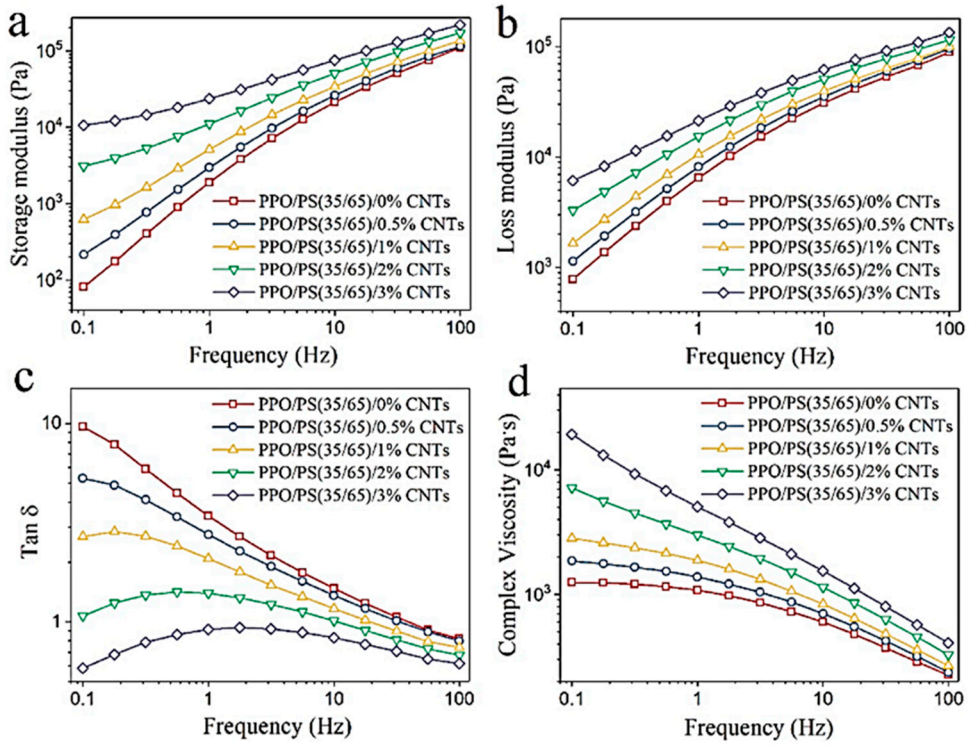

Figure 21. (a) Storage modulus, (b) loss modulus, (c) damping factor (tan δ), and (d) complex viscosity plotted against frequency for CNT-filled PPO/PS (35/65) blends with CNT concentrations of 0, 0.5, 1, 2, and 3 wt.% at a temperature of 270 °C [28].

Preprints.org (www.preprints.org) | NOT PEER-REVIEWED | Posted: 26 November 2024 doi:10.20944/preprints202411.1997.v1

Moskalyuk et al. [73] investigated the elastic properties of PS-based nanocomposites filled with inclusions such as SiO_2, Al_2O_3, alumosilicates, and carbon nanofillers. Composites were fabricated using melt technology, and linear and non-linear elastic properties were studied. The addition of rigid fillers significantly increased the elastic modulus, with carbon fillers achieving up to an 80% rise. Non-linear elastic moduli were more sensitive to filler content than linear ones. Figure 22 (a) shows the elastic modulus as a function of filler type and concentration, highlighting those carbon-based fillers significantly improved elasticity. Marcourt et al. [74] studied CNT-filled conductive polymer composites (CPCs) using pure PS and high-impact polystyrene (HIPS). They employed a volume segregation strategy to achieve conductivity at low CNT content by maintaining a continuous filler phase. The study monitored electrical conductivity and elongational stress, showing that both composites behaved similarly during CNT network destruction, and the HIPS nodules slightly hindered the structuring during deformation. Figure 22. (b) shows storage modulus (G') vs. frequency for PS composites, and Figure 22. (c) for HIPS composites, highlighting higher modulus in HIPS due to rubber nodules. Figure 22. (d) illustrates equilibrium modulus vs. filler concentration, where PS follows a percolation exponent of 2.76, while HIPS exhibits a lower exponent of 1.84, indicating a different network structure.

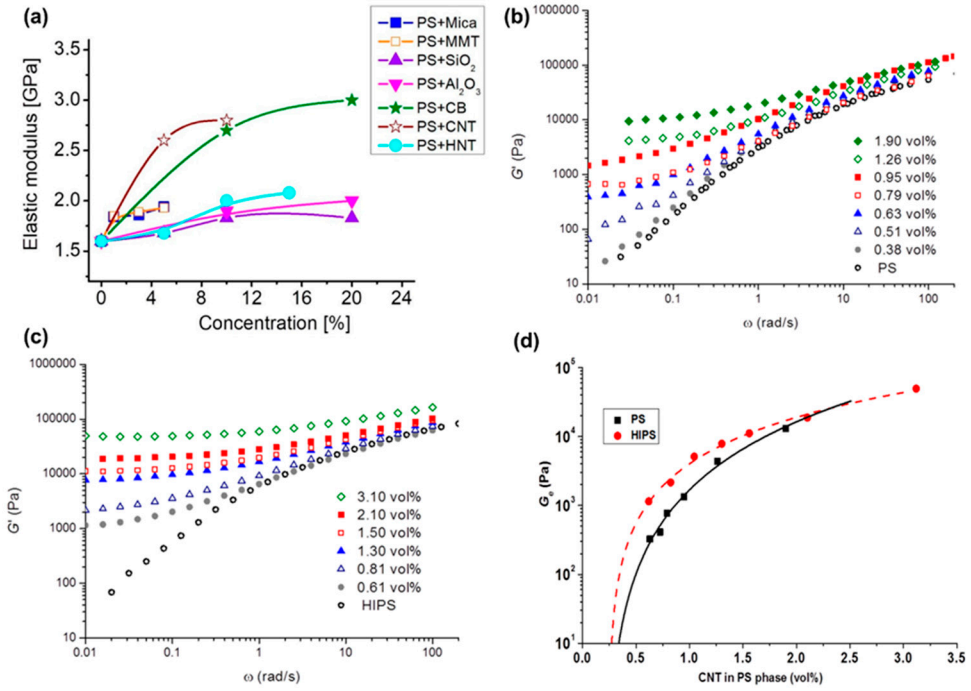

Figure 22. (a) Elastic modulus of PS composites relative to filler concentration [73]. (b) Storage modulus as a function of angular frequency at 200°C for PS-based composites at varying CNT concentrations. (c) Storage modulus as a function of angular frequency at 200°C for HIPS composites, with volume concentrations specified for the PS phase. (d) Equilibrium modulus plotted against CNT volume fraction in the PS continuous phase. Symbols represent experimental results, while lines correspond to predictions from percolation theory [74].

4.3. Shear Thinning and Flow Behavior

Shear thinning, or pseudoplastic behavior, is a phenomenon where the viscosity of a material decreases with increasing shear rate. This behavior is commonly observed in PS/CNT composites, particularly at high CNT concentrations. The shear thinning behavior is attributed to the alignment of CNT under shear forces, which reduces the internal friction and resistance to flow. The flow behavior of PS/CNT composites can be characterized using the power-law model, which relates shear stress (τ) to shear rate (γ) by the following equation:

$$\tau = K \gamma^{n} \quad (4)$$

 doi:10.20944/preprints202411.1997.v1

where "K" is the consistency index and "n" is the flow behavior index. In the case of shear-thinning materials, the flow behavior index "n" is less than 1, indicating a decrease in viscosity with increasing shear rate. The presence of CNT in the PS matrix affects the power-law parameters, with higher CNT concentrations typically leading to more pronounced shear thinning behavior. The shear thinning behavior of PS/CNT composites is advantageous in processing applications, as it allows for easier flow and moldability under high shear conditions. However, it also poses challenges in achieving uniform dispersion and controlling the material's final properties.

A study [22] investigated the effects of three types of styrene-butadiene block copolymers (SB and SBS) on the morphology, electrical, and rheological properties of immiscible polypropylene/ polystyrene (PP/PS) blends filled with MWCNT at a fixed ratio of 70:30 vol.%. Adding copolymers reduced droplet size in the blend and improved morphology, while MWCNT maintained its ability to create co-continuity. Notably, the electrical resistivity of the PP/PS/ 1.0 vol.% MWCNT system decreased by 5 orders of magnitude due to the formation of conductive networks through PS droplets, PP, and copolymer micelles. Molecular simulations indicated that di-block copolymers had better interactions with MWCNT than triblock copolymers, while interactions between copolymers and PP or PS were stronger than with MWCNT. TEM images showed that MWCNT localization shifted from PS to the PS–PP–micelle interfaces. Figure 23 displays shear viscosity as a function of shear rate for neat PP, PS, and copolymers, showing that PS has the lowest viscosity (597 Pa·s) compared to the copolymers. This lower viscosity likely facilitated better wetting of MWCNT, reducing their interaction with copolymers and PP. The study also used Hildebrand solubility parameters to analyze interactions among the copolymers, polymers, and MWCNT, highlighting the complexity of these relationships.

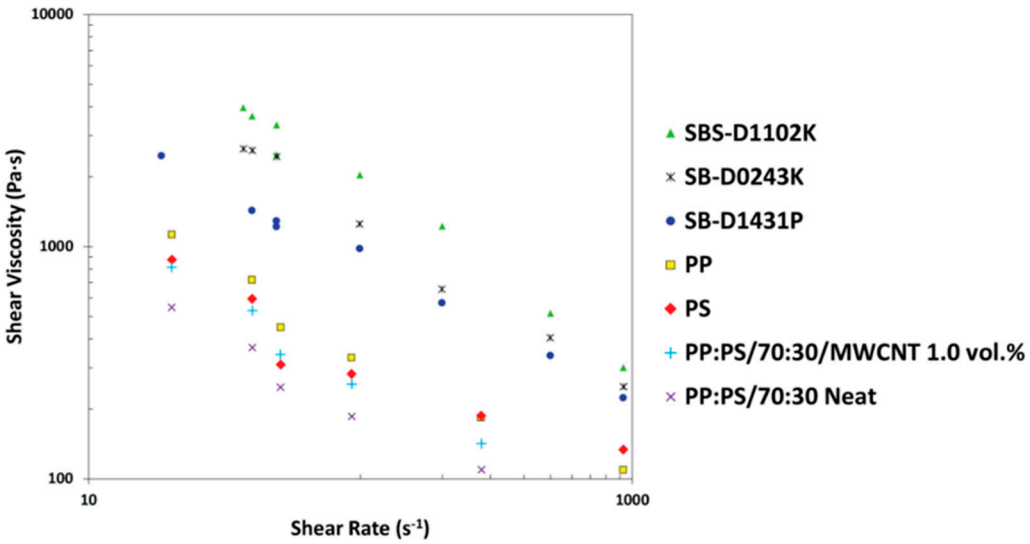

Figure 23. Shear viscosity as a function of shear rate for pure polypropylene (PP), pure polystyrene (PS), and pure styrene-butadiene block copolymers, measured using capillary rheology [22].

In another study [75] Massoudi and coauthors examined constitutive relations for flow and heat transfer in nanofluids, emphasizing the measurement of viscosity and thermal conductivity. It highlighted the limitations of conventional models, which often fail to account for non-linear and time-dependent behaviors. The research proposed treating nanofluids as generalized second-grade fluids, with viscosity dependent on the deformation rate. Key findings showed that solid concentration and fluid nonlinearity significantly influenced viscosity, and the proposed model effectively described fluid behavior compared to experimental data. Additionally, it noted that an orthogonal rheometer is required to assess the normal stress differences in nanofluids.

Kagarise et al. [76] conducted a detailed study on the transient shear rheology of PS composites reinforced with CNFs. Their findings demonstrated that as the concentration of CNFs increased, the stress overshot response to transient shear also became more pronounced. Additionally, the steady-state viscosity of the composites, observed at long times under constant shear, increased with higher

 doi:10.20944/preprints202411.1997.v1

CNF concentrations. These results highlighted the influence of CNFs on the viscoelastic properties of the composite, particularly under shear stress.

Figure 25 (a,b) presents the transient shear viscosity versus time for the composites at different constant shear rates. In Figure 25 (a), the pure PS (SC0) shows typical rheological behavior for a homogeneous linear polymer, exhibiting Newtonian characteristics at lower shear rates and shear thinning at higher rates. At shear rates of 0.01 s^{-1}, 0.001 s^{-1}, and 0.0001 s^{-1}, the viscosity curves overlap, indicating minimal change in viscosity with time. In contrast, Figure 25 (b) for the PS composite with 10 wt.% CNF (SC10) shows a more pronounced shear thinning effect at low shear rates (below 0.1 s^{-1}), where the viscosity significantly increases, demonstrating the strong influence of CNF content on the composite's rheological response. Figure 25 (c,d) illustrates the reduced stress at the startup of constant shear for both SC0 and SC10 composites, plotted as a function of strain. The reduced stress, τ_{red}, represents the ratio of transient shear stress to steady-state shear stress. Figure 25 (c) shows that the SC0 sample exhibits typical behavior with minimal stress overshoot at all shear rates. However, Figure 25 (d) reveals that in the SC10 sample, the magnitude of the stress overshoot increases with increasing shear rates, showcasing a much more pronounced viscoelastic response. Notably, the strain corresponding to the peak of the stress overshoot decreases as the shear rate increases in SC10, a behavior absents in SC0.

Additionally, the overshot width (the duration over which the stress exceeds steady-state levels) narrows with increasing shear rates in SC10, whereas it remains relatively constant for SC0. These differences between SC0 and SC10 indicate that the addition of CNFs significantly alters the structural dynamics of the composite during shear, leading to higher stress responses and enhanced shear thinning behavior. This finding suggests that CNFs play a crucial role in modifying the transient and steady-state rheological properties of PS-based composites.

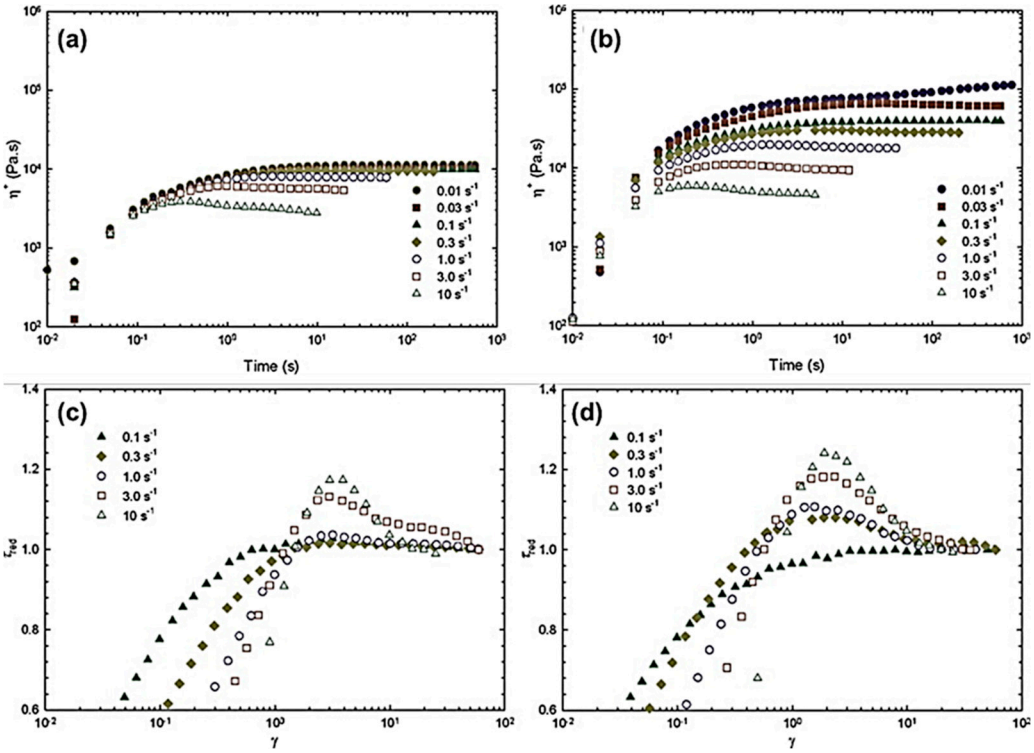

Figure 25. Transient shear viscosity as a function of time for (a) SC0 (pure PS) and (b) SC10 (PS with 10 wt.% CNF) composites at various constant shear rates. The respective shear rates are indicated in the legend for each plot. Reduced stress during the startup of constant shear for different shear rates in (c) SC0 (pure PS) and (d) SC10 (PS with 10 wt.% CNF) samples. The corresponding shear rates for each case are listed in the legend [76].

5. Challenges and Future Perspectives

Developing PS/CNT composites presents several intricate challenges that must be addressed to harness their potential in various applications fully. One of the most pressing issues is achieving a

 doi:10.20944/preprints202411.1997.v1

uniform dispersion of CNT within the PS matrix. The high surface area and strong van der Waals forces inherent to CNT often lead to significant aggregation, which can severely detract from the mechanical and rheological properties of the composite material. While techniques such as sonication, high-shear mixing, and functionalization have been employed to improve dispersion, each method has inherent limitations; for instance, sonication can induce fragmentation, and high-shear mixing may result in thermal degradation. Consequently, future research must focus on exploring innovative dispersion strategies, including advanced mechanical mixing techniques and the development of novel surfactants tailored for CNT stabilization, to achieve a more homogeneous distribution without compromising the integrity of the CNT.

Equally critical is the challenge of ensuring strong interfacial bonding between CNT and the PS matrix. The chemically inert and smooth surface of CNT can hinder effective stress transfer, thereby undermining the potential mechanical enhancements that these composites can offer. Functionalization of CNT serves as a common approach to enhance interfacial interactions; however, it may inadvertently alter the properties of the CNT, which can diminish their reinforcing capabilities. Thus, pursuing new functionalization methods that enhance compatibility while preserving the unique characteristics of CNT is vital. Additionally, exploring coupling agents and compatibilizers that promote better interactions between CNT and PS could improve composite performance.

Scalability and cost remain significant barriers to commercializing PS/CNT composites. The expense of producing high-quality CNT and the complexity of ensuring consistent dispersion and performance at an industrial scale present a terrible challenge. Ongoing research is focused on developing more cost-effective synthesis methods for CNT and optimizing processing conditions that enhance the feasibility of large-scale manufacturing to mitigate these issues. Furthermore, the environmental and health implications of CNT cannot be overlooked. Concerns regarding their toxicity to human health and ecosystems necessitate a concerted effort to develop safer, low-toxicity variants of CNT alongside improved handling and disposal methods.

Several targeted solutions can be implemented to address the challenges associated with the development of PS/CNT composites. Achieving uniform dispersion of CNT can be facilitated through advanced mixing techniques, such as combining high-energy ultrasonic mixing with high shear mixing to maintain CNT integrity. Developing and using novel surfactants specifically designed for CNT stabilization will further enhance dispersion without negatively impacting their properties. Employing in situ polymerization methods during the synthesis of PS may also promote improved CNT distribution. Optimizing functionalization techniques is crucial to ensuring strong interfacial bonding; this includes grafting polymer chains onto CNT surfaces and incorporating effective coupling agents that enhance compatibility with the PS matrix. Investigating hybrid composites that combine CNT with other nanofillers can also improve bonding and overall performance. Addressing scalability and cost concerns necessitates research into more cost-effective synthesis methods for CNT, such as using alternative precursors in chemical vapor deposition (CVD), while optimizing processing parameters for efficiency and quality. Collaborations between academia and industry can also foster knowledge sharing and resource utilization for scalable production. Developing low-toxicity CNT and comprehensive safe handling protocols is essential to mitigate environmental and health concerns.

Moreover, formulating biodegradable PS/CNT composites and conducting lifecycle assessments will help ensure environmental sustainability. Finally, leveraging interdisciplinary collaboration and computational tools is vital; promoting research initiatives integrating machine learning can accelerate the identification of optimal material formulations and processing conditions. Together, these solutions present a comprehensive approach to advancing the field of PS/CNT composites and realizing their full potential in various applications.

6. Conclusions

The rheological properties of PS/CNT composites are crucial for their processing and performance in advanced applications. Incorporating CNT significantly alters parameters such as viscosity, elasticity, and flow behavior, making uniform dispersion a critical challenge. Agglomeration due to strong van der Waals forces increases viscosity and reduces flowability, complicating processing methods. The interaction mechanisms, including Van der Waals forces,

covalent bonding, and π-π stacking, enhance viscoelastic properties and facilitate better stress transfer from the matrix to CNT, improving mechanical performance. Preparation methods, such as melt mixing, solution mixing, and others, significantly impact the rheological behavior, presenting unique advantages and limitations regarding CNT dispersion. PS/CNT composites typically exhibit shear thinning and viscoelastic characteristics, which are essential for extrusion and injection molding. Achieving the right balance between viscosity and elasticity is vital for effective material processing while maintaining the final product's integrity. This review highlights the current challenges and future directions in the field and is a valuable resource for new researchers. Our comprehensive collection of data and insights can guide future investigations, helping to foster innovation in the development and optimization of PS/CNT composites. By addressing existing challenges and leveraging this accumulated knowledge, the full potential of PS/CNT composites can be realized across various industries, including electronics, aerospace, and automotive engineering.

Author Contributions: Writing—original draft preparation, S.Y.; writing—review and editing, Z.A.; formal analysis and investigation, S.A.; revision and analysis, A.D. All authors have read and agreed to the published version of the manuscript.

Funding: This research received no external funding.

Institutional Review Board Statement: Not applicable.

Data Availability Statement: Not applicable

Informed Consent Statement: Not applicable.

Acknowledgments: Not applicable.

Conflicts of Interest: The authors declare no conflicts of interest.

References

1. Oladele, I.O.; Omotosho, T.F.; Adediran, A.A. Polymer-based composites: an indispensable material for present and future applications. *Int. J. Polym. Sci.* **2020**, *2020*, 8834518.
2. Kashfipour, M.A.; Mehra, N.; Zhu, J. A review on the role of interface in mechanical, thermal, and electrical properties of polymer composites. *Adv. Compos. Mater.* **2018**, *1*, 415-439.
3. Mergen, Ö.B.; Arda, E.; Evingür, G.A. Electrical, optical, and mechanical percolations of multi-walled carbon nanotube and carbon mesoporous-doped polystyrene composites. *J. Compos. Mater.* **2020**, *54*, 31-44.
4. Pantano, A. Mechanical properties of CNT/polymer. In *Carbon Nanotube-Reinforced Polymers*; Elsevier: 2018; pp. 201-232.
5. Li, H.; Wang, G.; Wu, Y.; Jiang, N.; Niu, K. Functionalization of Carbon Nanotubes in Polystyrene and Properties of Their Composites: A Review. *J. Polym.* **2024**, *16*, 770.
6. Park, J.S.; An, J.H.; Jang, K.-S.; Lee, S.J. Rheological and electrical properties of polystyrene nanocomposites via incorporation of polymer-wrapped carbon nanotubes. *KARJ* **2019**, *31*, 111-118.
7. Lee, J.; Kim, H. Rheological properties and phase structure of polypropylene/polystyrene/multiwalled carbon nanotube composites. *KARJ* **2020**, *32*, 153-158.
8. Khaksar, M.-R.; Ghazi-Khansari, M. Determination of migration monomer styrene from GPPS (general purpose polystyrene) and HIPS (high impact polystyrene) cups to hot drinks. *Toxicol. Mech. Methods.* **2009**, *19*, 257-261.
9. Alfarraj, A.; Nauman, E.B. Super HIPS: improved high impact polystyrene with two sources of rubber particles. *Polym. J.* **2004**, *45*, 8435-8442.
10. Ramli Sulong, N.H.; Mustapa, S.A.S.; Abdul Rashid, M.K. Application of expanded polystyrene (EPS) in buildings and constructions: A review. *J. Appl. Polym. Sci.* **2019**, *136*, 47529.
11. Aksit, M.; Zhao, C.; Klose, B.; Kreger, K.; Schmidt, H.-W.; Altstädt, V. Extruded polystyrene foams with enhanced insulation and mechanical properties by a benzene-trisamide-based additive. *Polym. J.* **2019**, *11*, 268.
12. Baugh, L.S.; Schulz, D.N. Discovery of syndiotactic polystyrene: its synthesis and impact. *Macromolecules* **2020**, *53*, 3627-3631.
13. Ali, Z.; Yaqoob, S.; Yu, J.; D'Amore, A. Critical review on the characterization, preparation, and enhanced mechanical, thermal, and electrical properties of carbon nanotubes and their hybrid filler polymer composites for various applications. *JCOMC* **2024**, 100434.
14. Dervishi, E.; Li, Z.; Xu, Y.; Saini, V.; Biris, A.R.; Lupu, D.; Biris, A.S. Carbon nanotubes: synthesis, properties, and applications. *JPST* **2009**, *27*, 107-125.

15. Kaseem, M.; Hamad, K.; Ko, Y.G. Fabrication and materials properties of polystyrene/carbon nanotube (PS/CNT) composites: a review. *Eur. Polym. J.* **2016**, *79*, 36-62.
16. Parnian, P.; D'Amore, A. Investigating the Electrical and Mechanical Properties of Polystyrene (PS)/Untreated SWCNT Nanocomposite Films. *J. Compos. Sci.* **2024**, *8*, 49.
17. Hoseini, A.H.A.; Arjmand, M.; Sundararaj, U.; Trifkovic, M. Significance of interfacial interaction and agglomerates on electrical properties of polymer-carbon nanotube nanocomposites. *Mater. Des.* **2017**, *125*, 126-134.
18. Wang, K.; Li, N.; Ren, K.; Zhang, Q.; Fu, Q. Exploring interfacial enhancement in polystyrene/multiwalled carbon nanotube monofilament induced by stretching. *Compos. - A: Appl. Sci. Manuf.* **2014**, *61*, 84-90.
19. Keshmiri, N.; Hoseini, A.H.A.; Najmi, P.; Liu, J.; Milani, A.S.; Arjmand, M. Highly conductive polystyrene/carbon nanotube/PEDOT: PSS nanocomposite with segregated structure for electromagnetic interference shielding. *Carbon* **2023**, *212*, 118104.
20. Khan, M.U.; Gomes, V.G.; Altarawneh, I.S. Synthesizing polystyrene/carbon nanotube composites by emulsion polymerization with non-covalent and covalent functionalization. *Carbon* **2010**, *48*, 2925-2933.
21. Erkmen, B. Polystyrene-based and carbon fabrİc-reİnforced polymer composİtes containing carbon nanotubes: preparation, modification and characterization. **2020**.
22. Navas, I.O.; Kamkar, M.; Arjmand, M.; Sundararaj, U. Morphology evolution, molecular simulation, electrical properties, and rheology of carbon nanotube/polypropylene/polystyrene blend nanocomposites: Effect of molecular interaction between styrene-butadiene block copolymer and carbon nanotube. *J. Polym.* **2021**, *13*.
23. Graves, K.A.; Higgins, L.J.; Nahil, M.A.; Mishra, B.; Williams, P.T. Structural comparison of multi-walled carbon nanotubes produced from polypropylene and polystyrene waste plastics. *JAAP* **2022**, *161*, 105396.
24. Shrivastava, N.K.; Khatua, B. Development of electrical conductivity with minimum possible percolation threshold in multi-wall carbon nanotube/polystyrene composites. *Carbon* **2011**, *49*, 4571-4579.
25. Shrivastava, N.; Maiti, S.; Suin, S.; Khatua, B. Influence of selective dispersion of MWCNT on electrical percolation of in-situ polymerized high-impact polystyrene/MWCNT nanocomposites. *EXPRESS Polym. Lett.* **2014**, *8*.
26. Mohd Nurazzi, N.; Asyraf, M.M.; Khalina, A.; Abdullah, N.; Sabaruddin, F.A.; Kamarudin, S.H.; Ahmad, S.b.; Mahat, A.M.; Lee, C.L.; Aisyah, H. Fabrication, functionalization, and application of carbon nanotube-reinforced polymer composite: An overview. *J. Polym.* **2021**, *13*, 1047.
27. Yousfi, M.; Alix, S.; Lebeau, M.; Soulestin, J.; Lacrampe, M.-F.; Krawczak, P. Evaluation of rheological properties of non-Newtonian fluids in micro rheology compounder: Experimental procedures for a reliable polymer melt viscosity measurement. *Polym. Test.* **2014**, *40*, 207-217.
28. Zhang, Q.; Wang, J.; Guo, B.-H.; Guo, Z.-X.; Yu, J. Electrical conductivity of carbon nanotube-filled miscible poly (phenylene oxide)/polystyrene blends prepared by melt compounding. *Compos. B Eng.* **2019**, *176*, 107213.
29. Papageorgiou, D.G.; Li, Z.; Liu, M.; Kinloch, I.A.; Young, R.J. Mechanisms of mechanical reinforcement by graphene and carbon nanotubes in polymer nanocomposites. *Nanoscale* **2020**, *12*, 2228-2267.
30. Erkmen, B.; Bayram, G. Influence of nanocomposite preparation techniques on the multifunctional properties of carbon fabric-reinforced polystyrene-based composites with carbon nanotubes. *SPE Polymers* **2022**, *3*, 163-175.
31. Sen, P.; Suresh, K.; Kumar, R.V.; Kumar, M.; Pugazhenthi, G. A simple solvent blending coupled sonication technique for synthesis of polystyrene (PS)/multi-walled carbon nanotube (MWCNT) nanocomposites: effect of modified MWCNT content. *Journal of Science: JS: AMD s* **2016**, *1*, 311-323.
32. Riolo, D.; Piazza, A.; Cottini, C.; Serafini, M.; Lutero, E.; Cuoghi, E.; Gasparini, L.; Botturi, D.; Marino, I.G.; Aliatis, I. Raman spectroscopy as a PAT for pharmaceutical blending: Advantages and disadvantages. *J. Pharm. Biomed. Anal.* **2018**, *149*, 329-334.
33. Azubuike, L.; Sundararaj, U. Interface strengthening of ps/apa polymer blend nanocomposites via in situ compatibilization: Enhancement of electrical and rheological properties. *J. Mater* **2021**, *14*, 4813.
34. Patole, A.S.; Patole, S.; Yoo, J.B.; Ahn, J.H.; Kim, T.H. Effective in situ synthesis and characteristics of polystyrene nanoparticle-covered multiwall carbon nanotube composite. *J. Polym. Sci., Part B: Polym. Phys.* **2009**, *47*, 1523-1529.
35. Rane, A.V.; Kanny, K.; Abitha, V.; Thomas, S. Methods for synthesis of nanoparticles and fabrication of nanocomposites. In *Synthesis of inorganic nanomaterials*; Elsevier: 2018; pp. 121-139.
36. Quijano, J.R.B. Mechanical, electrical and sensing properties of melt-spun polymer fibers filled with carbon nanoparticles. *TUD*, 2018.
37. Farha, F.I.; Wei, X.; Zhang, Q.; Liu, W.; Chen, W.; Liu, L.; Xu, F. Microstructural Tuning of Twisted Carbon Nanotube Yarns through the Wet-Compression Process: Implications for Multifunctional Textiles. *ACS Appl. Nano Mater.* **2022**, *5*, 11071-11079.

38. Zhao, X.; Kong, D.; Tao, J.; Kong, N.; Mota-Santiago, P.; Lynch, P.A.; Shao, Y.; Zhang, J. Wet Twisting in Spinning for Rapid and Cost-Effective Fabrication of Superior Carbon Nanotube Yarns. *Adv. Funct. Mater.* **2024**, 2400197.
39. Prasad, G.; Chakradhar, R.; Bera, P.; Anand Prabu, A. UV and thermally stable polystyrene-MWCNT superhydrophobic coatings. *SIA* **2017**, *49*, 93-98.
40. Zhou, X.; Zhu, Y.; Liang, J.; Yu, S. New fabrication of Styrene-Butadiene Rubber/Carbon Nanotubes nanocomposite and corresponding mechanical properties. *J. Mater. Sci. Technol.* **2010**, *26*, 1127.
41. Tambe, S.; Jain, D.; Meruva, S.K.; Rongala, G.; Juluri, A.; Nihalani, G.; Mamidi, H.K.; Nukala, P.K.; Bolla, P.K. Recent advances in amorphous solid dispersions: preformulation, formulation strategies, technological advancements and characterization. *Pharmaceutics* **2022**, *14*, 2203.
42. Ozmen, L.; Langrish, T. A study of the limitations to spray dryer outlet performance. *Dry. Technol.* **2003**, *21*, 895-917.
43. Byun, S.; Lee, J.; Lee, J.; Jeong, S. Reusable carbon nanotube-embedded polystyrene/polyacrylonitrile nanofibrous sorbent for managing oil spills. *Desalination* **2022**, *537*, 115865.
44. Parangusan, H.; Ponnamma, D.; Hassan, M.K.; Adham, S.; Al-Maadeed, M.A.A. Designing carbon nanotube-based oil absorbing membranes from gamma irradiated and electrospun polystyrene nanocomposites. *J. Mater.* **2019**, *12*, 709.
45. Oliveira, E.Y.; Bode, R.; Escárcega-Bobadilla, M.V.; Zelada-Guillén, G.A.; Maier, G. Polymer nanocomposites from self-assembled polystyrene-grafted carbon nanotubes. *New J Chem* **2016**, *40*, 4625-4634.
46. Liu, Y.; Wang, G.-J. A novel method for well-organized polystyrene-grafted multi-walled carbon nanotube bundles via self-assembly in tetrahydrofuran. *Fibers Polym.* **2013**, *14*, 1073-1081.
47. Zhang, C.; Liu, T.; Lu, X. Facile fabrication of polystyrene/carbon nanotube composite nanospheres with core-shell structure via self-assembly. *Polym. J.* **2010**, *51*, 3715-3721.
48. Song, J.; Wang, F.; Yang, X.; Ning, B.; Harp, M.G.; Culp, S.H.; Hu, S.; Huang, P.; Nie, L.; Chen, J. Gold nanoparticle coated carbon nanotube ring with enhanced raman scattering and photothermal conversion property for theranostic applications. *J. Am. Chem. Soc.* **2016**, *138*, 7005-7015.
49. Lv, Q.; Tao, X.; Shi, S.; Li, Y.; Chen, N. From materials to components: 3D-printed architected honeycombs toward high-performance and tunable electromagnetic interference shielding. *Compos B Eng* **2022**, *230*, 109500.
50. Baskakova, K.I.; Okotrub, A.V.; Bulusheva, L.G.; Sedelnikova, O.V. Manufacturing of carbon nanotube-polystyrene filament for 3D printing: nanoparticle dispersion and electromagnetic properties. *J. Nanoeng. Nanomanuf.* **2022**, *2*, 292-301.
51. Zheng, Y.; Huang, X.; Chen, J.; Wu, K.; Wang, J.; Zhang, X. A review of conductive carbon materials for 3D printing: Materials, technologies, properties, and applications. *J. Mater.* **2021**, *14*, 3911.
52. Hong, J.; Han, J.Y.; Yoon, H.; Joo, P.; Lee, T.; Seo, E.; Char, K.; Kim, B.-S. Carbon-based layer-by-layer nanostructures: from films to hollow capsules. *Nanoscale* **2011**, *3*, 4515-4531.
53. Srivastava, S.; Kotov, N.A. Composite layer-by-layer (LBL) assembly with inorganic nanoparticles and nanowires. *Acc. Chem. Res.* **2008**, *41*, 1831-1841.
54. Zhang, X.; Chen, H.; Zhang, H. Layer-by-layer assembly: from conventional to unconventional methods. *ChemComm* **2007**, 1395-1405.
55. Harish, M. Processing and study of carbon nanotube/polymer nanocomposites and polymer electrolyte materials. **2007**.
56. Lubineau, G.; Rahaman, A. A review of strategies for improving the degradation properties of laminated continuous-fiber/epoxy composites with carbon-based nanoreinforcements. *Carbon* **2012**, *50*, 2377-2395.
57. Liao, C.-H.; Hung, P.-S.; Cheng, Y.; Wu, P.-W. Combination of microspheres and sol-gel electrophoresis for the formation of large-area ordered macroporous SiO_2. *Electrochem. commun.* **2017**, *85*, 6-10.
58. Gao, B.; Chen, G.Z.; Puma, G.L. Carbon nanotubes/titanium dioxide ($CNTs/TiO_2$) nanocomposites prepared by conventional and novel surfactant wrapping sol–gel methods exhibiting enhanced photocatalytic activity. *Appl. Catal., B* **2009**, *89*, 503-509.
59. Toyama, N.; Takahashi, T.; Terui, N.; Furukawa, S. Synthesis of polystyrene@ TiO_2 core–shell particles and their photocatalytic activity for the decomposition of methylene blue. *Inorganics* **2023**, *11*, 343.
60. Lai, H.; Zhao, Z.; Yu, W.; Lin, Y.; Feng, Z. Physicochemical and Antibacterial Evaluation of TiO_2/CNT Mesoporous Nanomaterials Prepared by High-Pressure Hydrothermal Sol–Gel Method under an Ultrasonic Composite Environment. *Molecules* **2023**, *28*, 3190.
61. Modan, E.M.; PLĂIAȘU, A.G. Advantages and disadvantages of chemical methods in the elaboration of nanomaterials. *The Annals of "Dunarea de Jos" University of Galati. Fascicle IX, Metallurgy and Materials Science* **2020**, *43*, 53-60.
62. Xie, Y.; Li, Z.; Tang, J.; Li, P.; Chen, W.; Liu, P.; Li, L.; Zheng, Z. Microwave-assisted foaming and sintering to prepare lightweight high-strength polystyrene/carbon nanotube composite foams with an ultralow percolation threshold. *J. Mater. Chem. C* **2021**, *9*, 9702-9711.

63. Xie, Y.; Tang, J.; Ye, F.; Liu, P. Microwave-assisted sintering to rapidly construct a segregated structure in low-melt-viscosity poly (lactic acid) for electromagnetic interference shielding. *ACS omega* **2020**, *5*, 26116-26124.
64. Shahbazi, M.; Aghvami-Panah, M.; Panahi-Sarmad, M.; Seraji, A.A.; Zeraatkar, A.; Ghaffarian Anbaran, R.; Xiao, X. Fabricating bimodal microcellular structure in polystyrene/carbon nanotube/glass-fiber hybrid nanocomposite foam by microwave-assisted heating: a proof-of-concept study. *J. Appl. Polym. Sci.* **2022**, *139*, 52125.
65. Baghel, P.; Sakhiya, A.K.; Kaushal, P. Ultrafast growth of carbon nanotubes using microwave irradiation: characterization and its potential applications. *Heliyon* **2022**, *8*.
66. Granados-Martínez, F.G.; Domratcheva-Lvova, L.; Flores-Ramírez, N.; García-González, L.; Zamora-Peredo, L.; Mondragón-Sánchez, M.d.L. Composite films from polystyrene with hydroxyl end groups and carbon nanotubes. *Mater. Res.* **2017**, *19*, 133-138.
67. Guzenko, N.; Godzierz, M.; Kurtyka, K.; Hercog, A.; Nocoń-Szmajda, K.; Gawron, A.; Szeluga, U.; Trzebicka, B.; Yang, R.; Rümmeli, M.H. Flexible Piezoresistive Polystyrene Composite Sensors Filled with Hollow 3D Graphitic Shells. *J. Polym.* **2023**, *15*, 4674.
68. Vodnik, V.V.; Dzunuzovic, E.; Dzunuzovic, J. Synthesis and characterization of polystyrene based nanocomposites. *Polystyrene: Synthesis, Characteristics and Applications, 1st ed.; Lynwood, C., Ed* **2014**, 201-240.
69. CARREAU, P.J. RHEOLOGY OF POLYMERS WITH NANOFILLERS. **2010**.
70. Park, S.-D.; Han, D.-H.; Teng, D.; Kwon, Y. Rheological properties and dispersion of multi-walled carbon nanotube (MWCNT) in polystyrene matrix. *Curr. Appl. Phys.* **2008**, *8*, 482-485.
71. Jarali, C.S.; Patil, S.F.; Pilli, S.C.; Lu, Y.C. Modeling the effective elastic properties of nanocomposites with circular straight CNT fibers reinforced in the epoxy matrix. *J. Mater. Sci.* **2013**, *48*, 3160-3172.
72. Fragneaud, B.; Masenelli-Varlot, K.; Gonzalez-Montiel, A.; Terrones, M.; Cavaille, J.-Y. Mechanical behavior of polystyrene grafted carbon nanotubes/polystyrene nanocomposites. *Compos. Sci. Technol.* **2008**, *68*, 3265-3271.
73. Moskalyuk, O.A.; Belashov, A.V.; Beltukov, Y.M.; Ivan'kova, E.M.; Popova, E.N.; Semenova, I.V.; Yelokhovsky, V.Y.; Yudin, V.E. Polystyrene-based nanocomposites with different fillers: Fabrication and mechanical properties. *J. Polym.* **2020**, *12*, 2457.
74. Marcourt, M.; Cassagnau, P.; Fulchiron, R.; Rousseaux, D.; Lhost, O.; Karam, S. High Impact Polystyrene/CNT nanocomposites: Application of volume segregation strategy and behavior under extensional deformation. *J. Polym.* **2018**, *157*, 156-165.
75. Massoudi, M.; Phuoc, T.X. Remarks on constitutive modeling of nanofluids. *Adv. Mech. Eng.* **2012**, *4*, 927580.
76. Kagarise, C.; Xu, J.; Wang, Y.; Mahboob, M.; Koelling, K.W.; Bechtel, S.E. Transient shear rheology of carbon nanofiber/polystyrene melt composites. *J. Nonnewton. Fluid Mech.* **2010**, *165*, 98-109.